# TESTING THE IMPORTANCE OF THE 4TH CTTC MOTIF FOR MYCORRHIZAL INDUCED *SIGRAS18* EXPRESSION

**Èlia Sans i Rillo**

**TREBALL FINAL DE GRAU BIOTECNOLOGIA**

**Academic tutor**: Dra. Dania García Sánchez, Basic Medical Sciences Department, URV (dania.garcias@urv.cat)

**In cooperation with**: Karlsruhe Institute of Technology (KIT)

**Professional tutor**: Prof. Dr. Natalia Requena, Molecular Phytopathology Department, KIT (natalia.requena@kit.edu)

3rd September 2025

I, Èlia Sans i Rillo, with DNI 48139390E, am aware of the guide to the prevention of plagiarism at the URV Prevention, detection and treatment of plagiarism in teaching: student guide (approved in July 2017) (http://www.urv.cat/ca/vidacampus/serveis/crai/que-us-oferim/formacio_competencies-nuclears/plagiarism/) and I affirm that this TFG (Bachelor Thesis) does not constitute any of the behaviours considered plagiarism by the URV.

Tarragona, 3rd September 2025

***"Symbiogenesis was the moon that pulled the tide of life from its oceanic depths to dry land and up into the air."***

— Lynn Margulis, *Symbiotic Planet* (1998)

## Acknowledgments

I would like to show my gratitude to Natalia for answering my last-minute call giving me the opportunity to be part of the lab, and for your warm welcome.

My gratitude also to Diana, who answered all my endless questions with patience, guided me through all the steps in the lab, and even took me to the long-desired botanical garden.

I would like to sincerely thank Dania for trusting me from the very first moment I asked her to be my tutor, and for encouraging me when I was unsure about everything at the beginning of the project.

A huge thank you to my family and friends who have always encouraged me and even came to visit me at the gateway to the *Schwarzwald*, at Karlsruhe.

# Index

## Details of the centre

This bachelor's degree final project was carried out during my internship at Karlsruhe Institute of Technology (KIT) between July and September 2024, as part of Diana Schwarz's doctoral research. Her research focuses on GRAS transcription factors in root development during arbuscular mycorrhizal symbiosis.

**Name of the centre**: Joseph Gottlieb Kölreuter Institute for Plant Sciences of KIT

**Area**: Molecular Phytopathology Department

**Adress**: Fritz-Haber-Weg 4, Building 30.43, 2nd Floor, D-76131 Karlsruhe, Germany

**Head of department and professional tutor**: Prof. Dr. Natalia Requena

**Contact details**: +49-721-608-44626 / natalia.requena@kit.edu

## Figure index

## Table index



## Abbreviations

**AM**: arbuscular mycorrhiza

**AMF**: arbuscular mycorrhizal fungi

**CSSP**: common symbiosis signalling pathway

**GA**: gibberellin (gibberellic acid)

**PAM**: periarbuscular membrane

**SL**: strigolactone

**TF**: transcription factor

## Summary

Arbuscular mycorrhiza (AM) is an ancient symbiosis between most land plants and AM fungi, which enhances plant nutrition, stress tolerance and resistance to pathogens, while fungi obtain fixed carbon from the host plant. This symbiosis essential in agriculture is tightly regulated through a complex exchange of signals, which leads to the reprogramming of development and metabolism in root arbuscule-containing cells. Some members of the GRAS transcription factor (TF) family are induced upon mycorrhization and play a crucial role in arbuscle accommodation. A great number of them possess a CTTC motif, a cis-regulatory element present in several mycorrhizal-induced TF.

In this study, a GUS promoter truncation assay was conducted to contribute to a better understanding of the regulation of the *SlGRAS18* TF, which is known to act as a negative regulator of arbuscule formation. The results show that a 240 bp fragment upstream of the *SlGRAS18* start codon, containing the 4$^{th}$ CTTC motif, is sufficient to induce its expression, suggesting that this motif may play a key role in the regulation of *SlGRAS18* under AM conditions.

**Keywords**: arbuscular mycorrhiza, *Solanum lycopersicum,* GRAS transcription factors, *SlGRAS18*, CTTC motif, cell reprogramming, GUS promoter truncation assay.

## Resum

Les endomicorrizes són una antiga simbiosi entre la majoria de les plantes terrestres vasculars i els fongs formadors d'arbuscles intracel·lulars en les arrels. Aquesta interacció millora la nutrició de les plantes, la tolerància a l'estrès abiòtic i la resistència a patògens, mentre que els fongs obtenen carboni fixat de la planta hoste. La simbiosi micorrízica està estretament regulada mitjançant un intercanvi complex de senyals, que condueix a la reprogramació del desenvolupament i el metabolisme de les cèl·lules radicals que contenen arbuscles. Alguns factors de transcripció (FT) de la família GRAS són induïts durant la micorrització i tenen un paper crucial en l'acomodació de l'arbuscle. Una gran part d'aquests conté el motiu CTTC, un element regulador cis present en diferents FT induïts per la pròpia micorrització.

En aquest estudi, es va dur a terme un assaig GUS amb truncament de promotor per a contribuir a una millor comprensió de la regulació del FT *SlGRAS18*, conegut per actuar com a regulador negatiu de la formació d'arbuscles. Els resultats mostren que un fragment de 240 pb *upstream* del codó d'inici de *SlGRAS18*, que conté el 4t motiu CTTC, és suficient per a induir la seva expressió. Aquest fet suggereix que el 4t motiu CTTC pot exercir un paper clau en la regulació de SlGRAS18 quan l'hoste es troba en una simbiosi arbuscular.

**Paraules clau**: micorriza arbuscular, *Solanum lycopersicum,* factors de transcripció GRAS, *SlGRAS18*, motiu CTTC, reprogramació cel·lular, assaig GUS amb truncament del promotor.

# 1. INTRODUCTION

One of the major challenges of modern agriculture is feeding the world's rapidly growing population in a sustainable way over time. The Green Revolution which took place between the 1940s and 1960s, while it succeeded in increasing food production, promoted practices such as over-fertilisation that have led to negative consequences for the environment, soil health, food security, and human well-being (Wang et al., 2024).

A significant portion of fertilisers is not absorbed by plants and leaches into groundwater, polluting it and causing eutrophication in aquatic systems. This leads to excessive algal growth that depletes dissolved oxygen necessary for the life of many other species in the ecosystem. In addition, the production of such fertilisers releases various greenhouse gases, such as $CO_2$, $CH_4$, or $N_2O$, the latter having a global warming potential 310 times greater than $CO_2$. When fertilisers are applied disproportionately, imbalances are created between essential macronutrients, leading to a deficiency of micronutrients. Another consequence of excessive fertiliser use is the degradation of soil structure, which reduces its capacity to retain nutrients, favouring their leaching. High nutrient concentrations also reduce mycorrhizal colonisation of roots and inhibit nitrogen fixation by *Rhizobium* bacteria (Jote, 2023).

Partly in response to these consequences, the European Commission has promoted the Farm to Fork strategy, one of the key pillars of the European Green Deal action plan. This initiative aims to facilitate the transition towards a sustainable food system to ensure access to healthy diets while protecting ecosystems. To this end, targets have been set, for instance, to reduce nutrient losses by at least 50% and to cut fertiliser use by 20% by 2030 (Salazar, 2023). One of the approaches to achieving these goals is to focus on soil health and its interactions with the plants and microorganisms that inhabit it. As an alternative to conventional fertilisers, biofertilisers are presented as substances containing living micro-organisms that, in association with roots, can enhance nutrient uptake by plants and improve soil quality (Tharanath et al., 2024; Wang et al., 2024).

Soil is not a merely physical support for plants but a complex and dynamically interconnected web of life. It harbours extremely complex biological communities, composed of hundreds to thousands of species of bacteria, fungi, archaea, nematodes, oomycetes, protists, and viruses. Just 1 g of soil can contain between $10^8$ and $10^{10}$ microbial cells (Custódio et al., 2022). It is estimated that 80% to 90% of the processes

occurring in soil are mediated by microorganisms, including soil structuring, nutrient recycling, mineral nutrient release, and the enhancement of plant functions (Custódio et al., 2022; Tharanath et al., 2024). Therefore, soil health is fundamental to the sustainable development of agriculture, and the integration of soil science into plant science research and crop improvement is crucial.

Understanding what shapes microbial communities in soil is essential, since they hold key ecosystem functions relevant to agriculture. However, soil diversity and composition are influenced by various abiotic and biotic factors. Abiotic factors include soil structure, moisture, pH or temperature (Custódio et al., 2022). In terms of biotic factors, interactions between soil organisms can be cooperative, competitive, or parasitic. Cooperative interactions can be further classified into mutualism or commensalism, depending on whether there is a reciprocal or unidirectional benefit, respectively (Tharanath et al., 2024).

In mutualistic plant-microorganism interactions, plant roots contribute to the formation of soil structure and provide organic matter that supports microbial growth. Additionally, plants exude a variety of organic compounds through the roots into the rhizosphere, the narrow zone of soil surrounding the roots. Through these exudates, the plant not only nourishes the microbial community in the rhizosphere, but also modulates it, as they serve as signalling molecules (Tharanath et al., 2024).

In return, soil microorganisms increase the plant acquisition of nutrients, for instance, through biological fixation of nitrogen. Additionally, mycorrhizal networks extend the absorbing surface up to 700%, growing in every direction, efficiently exploring the soil, and increasing plant uptake of nitrogen, phosphorus, sulphur, immobile micronutrients such as copper and zinc, and other soil-derived mineral cations (Tharanath et al., 2024; Wang et al., 2024). The microbial community can also influence root architecture and function, promoting plant growth and development. Such interactions are crucial for plant competitiveness and survival in natural ecosystems (Custódio et al., 2022), and have a great potential for improving agricultural sustainability by reducing fertiliser dependence and enhancing crop resilience to environmental and biological stress.

### 1.1 Root organisation

The root is the first embryonic organ to sprout from the seed. It has an elongated shape and positive geotropism, this mean, it grows in the direction of gravitational pull, towards

the centre of the soil. Its main functions are to anchor the plant to the substrate and absorb nutrients in solution. In addition, it transports water and nutrients axially to the stem and leaves, as well as photosynthates from the leaves back to the root, and can establish symbiotic associations with soil microorganisms (Paniagua, 2011).

Root elongation (primary growth) of the root leads to the formation of its fundamental tissues and structures, which are represented in Figure 1. The outermost layer of the primary structure is the epidermis (or rhizodermis), which consists of a single row of epidermal cells. This layer lacks a cuticle and produces radical hairs, which are key in the absorption of water and nutrients (Lynch et al., 2021; Paniagua, 2011).

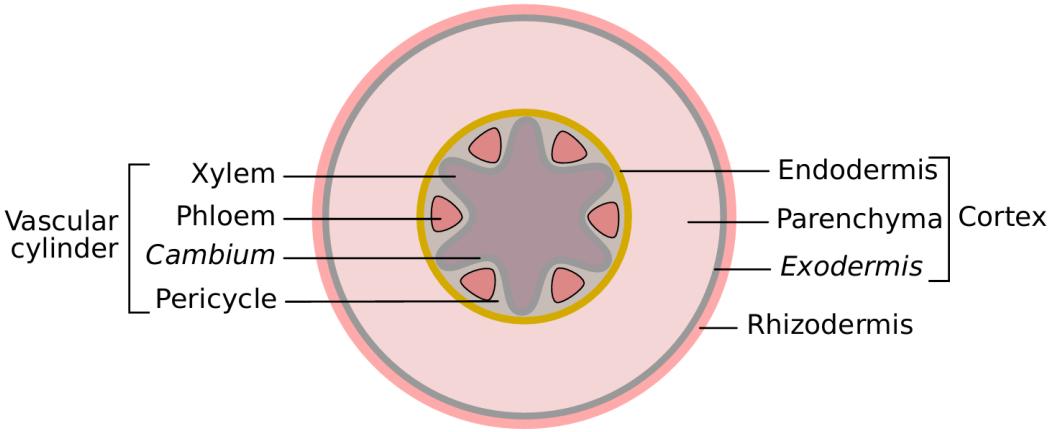


**Figure 1.** Cross-section through the maturation zone of a root, showing the primary structure. Schematic representation of root anatomy showing the primary tissue layers: rhizodermis or epidermis, cortex (including exodermis, parenchyma or inner cortex, and endodermis), and vascular or central cylinder (composed of pericycle, cambium, phloem, and xylem). In the representation, xylem and phloem are shown as a homogeneous mass. It should be noted that they are made up of different vascular vessels. From Shipunov **(2021)**.

Contiguous to the epidermis lies the cortex, a parenchymatous tissue that forms during primary development and accumulates storage substances, mainly starch. In some dicotyledonous species, the cortex can be divided into three zones: exodermis, inner cortex (parenchyma), and endodermis (Lynch et al., 2021; Paniagua, 2011). It is within both the cortex and epidermis where the association with mycorrhizal fungi takes place (Shi et al., 2023).

The central cylinder is located behind the endodermis and is the innermost part of the root. It is primarily responsible for transport and comprises the pericycle and the vascular vessels. The pericycle is the next layer after the endodermis and consists of living cells that possess the meristematic potential to generate lateral roots. Beneath the pericycle lie the vascular bundles composed by the xylem and the phloem. Xylem, arranged in a radial

pattern, is responsible for transporting water and nutrient, while phloem, interspersed between the xylem bundles, conducts the photosynthates. (Paniagua, 2011).

The primary structure allows the root to efficiently explore the soil and absorb resources. Unlike monocots, which usually maintain their primary structure throughout their lives, dicots (and gymnosperms) undergo significant secondary growth that thickens the root. Thus, older roots increase transport capacity and provide mechanical support and resistance against pathogens and herbivores (Lynch et al., 2021; Paniagua, 2011).

This growth is due to the activity of a secondary meristematic tissues called the vascular cambium (Figure 1) and, more externally, the phellogen (also known as cork cambium). The latter is found in the cortex and produces suber (cork) and phelloderm (non-suberified parenchymatous tissue), which function as a protective layer and replace the primary epidermis and cortex (Paniagua, 2011).

This replacement of primary tissues by secondary tissues prevents symbiosis to occur with arbuscular mycorrhizal fungi (AMF). For this reason, thinner and younger roots, which are usually lateral roots or root tips, show higher rates of mycorrhizal colonisation (Paniagua, 2011). Under certain stress conditions, such as phosphorus deficiency, secondary root growth is suppressed, which prolongs the window for arbuscular mycorrhizal (AM) symbiosis. This suppression appears to be an adaptive strategy to improve the metabolic efficiency of soil exploration and phosphorus uptake, allowing for greater longitudinal root growth rather than radial thickening (Lynch et al., 2021).

The morphology and physiology of the root system are influenced not only by the regulation of phytohormones such as gibberellins, cytokinins, auxins or ethylene, but also by a wide range of abiotic and biotic factors in the rhizosphere. Both the availability and composition of soil nutrients, as well as the symbiosis with microorganisms, can lead to huge modifications in root organisation, enabling the plant to adapt better to changing environmental conditions (Lynch et al., 2021).

### 1.2 Arbuscular mycorrhizal symbiosis

Mycorrhizas are mutualistic symbiotic associations established between soil fungi and the roots of approximately 80-90% of terrestrial plant species. These interactions are based on the reciprocal exchange of nutrients and are considered one of the most important inter-kingdom biological relationships. The first mycorrhizas, which date back

more than 450 million years, played an essential role in the terrestrial colonisation of the first plants as arbuscular mycorrhizas. Since then, mycorrhizal lineages have diversified and adapted to climatic changes. Mycorrhizas continue to adapt to changing environmental conditions, including those imposed by the Anthropocene (Brundrett & Tedersoo, 2018; Genre et al., 2020; Smith & Read, 2008).

There are four main types of mycorrhizas, which differ in their morphological characteristics and the groups of plants and fungi involved: arbuscular mycorrhizas, ectomycorrhizas, ericoid mycorrhizas, and orchid mycorrhizas. See Annex 1 for further details on this topic.

The most common and widespread type of mycorrhiza in nature are AM, occurring in over 80% of terrestrial plant species (Rui et al., 2022). Fungi involved in AM symbiosis belong to the subphylum Glomeromycotina within the phylum Mucoromycota. This sort of symbiosis is characterised by the presence of arbuscules (Figure 2B), highly branched structures formed inside root cortex cells, which are specialised for nutrient exchange (Genre et al., 2020).

### 1.2.1 Lifecycle of AM fungi

AMF establish a network of hyphae both inside the host plant roots (intraradical mycelium) and in the surrounding soil (extraradical mycelium) (Smith & Read, 2008). These fungi are obligate symbionts or obligate biotrophs, meaning they are metabolically dependent on a living plant host to complete their life cycle under natural conditions. On the one hand, AMF are auxotroph for some lipids, that is, they lack the genetic machinery for *de novo* biosynthesis of long-chain fatty acids and rely entirely on the host plant to supply these compounds (Kameoka & Gutjahr, 2022). On the other hand, while spores can germinate and grow into the soil, this initial growth relies on reserves within the spore. For sustained growth, proliferation, and the production of new spores, the fungus requires successful colonisation of a host root system (Cargill et al., 2025; Choi et al., 2018).

When a compatible fungus is nearby, host plant releases signal molecules, primarily, strigolactones (SLs). SLs are hormones that stimulate spore germination and hyphal branching in AMF (Rui et al., 2022). The same way, the fungus releases Myc (mycorrhizal) factors, namely lipochitooligosaccharides and short chitin oligomers, which are perceived by the plant. Both organisms communicate via oligosaccharides and butenolides (Choi et al., 2018; Ho-Plágaro & García-Garrido, 2022a).

The perception of Myc factors released by the AM fungus triggers a nuclear calcium spiking in the epidermis of the host plant to activate the common symbiosis signalling pathway (CSSP). The CSSP is a crucial regulatory pathway for AM symbiosis, which orchestrates gene expression necessary for epidermal penetration and subsequent symbiotic development (Ho-Plágaro & García-Garrido, 2022a).

Following this reciprocal recognition, both organisms prepare for the symbiosis. Fungal hyphae form specialized foot-like attachment structures called hyphopodia on the root epidermis (Figure 2A.1). The formation of these structures is influenced by contact recognition and is a prerequisite for successful root colonisation (Cargill et al., 2025; Choi et al., 2018; Smith & Read, 2008).

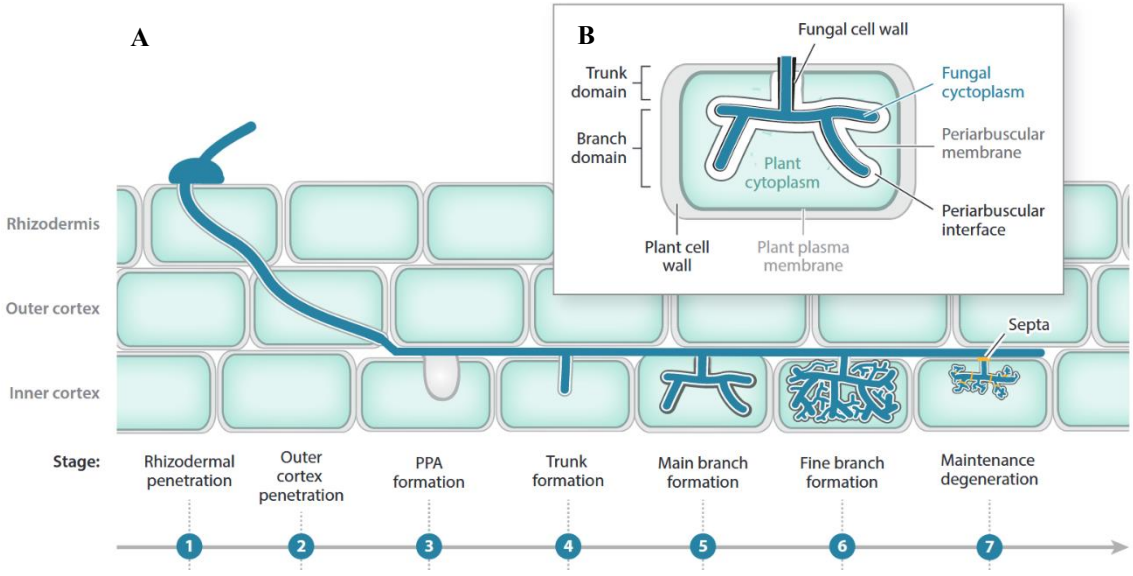


**Figure 2.** Steps of AM fungal colonisation of a host plant root. (A.1) Fungal attachment structures, called hyphopodia, form on the cell surface while the host cell produces a prepenetration apparatus (PPA) in the rhizodermis to intracellularly accommodate the fungus. (A.2) Fungal hyphae grow radially toward the inner cortex to initiate arbuscule formation. (A.3) Fungal hyphae grow longitudinally and PPA are prepared in the inner cortex for arbuscule accommodation. Arbuscule development can be divided into five substages featuring development and collapse of arbuscules (stages A.3-7). (B) Accommodation of the AM fungus by the inner cortex cell implies the formation of the periarbuscular membrane (PAM), which is a specialized extension of the host plant plasma membrane. The PAM and the AM fungus plasma membrane delimit the periarbuscular space or interface, where the nutrient and signal exchange occurs. Adapted from Choi et al. (2018).

Simultaneously, the plant actively prepares for fungal entry by forming a prepenetration apparatus (PPA), a transient, tube-like intracellular infection structure within its epidermal cells (Figure 2A.1-3). This structure essentially defines the future intracellular path of hyphal penetration. The PPA consists of an invaginated plasma membrane supported by an extensive network of the endoplasmic reticulum and cytoskeleton material. Once the PPA is produced, local softening of the plant cell wall on the contact site is assumed to allow epidermal penetration by AM fungal hyphae. The formation of

the PPA is a major cellular reorganization requiring symbiosis-specific gene expression. The entire process of PPA formation and hyphal crossing of the epidermis can take 7-8 hours (Genre et al., 2005).

Following epidermal penetration, fungal hyphae proliferate inter- and intracellularly through the outer and inner cortical layer via PPA-related intracellular accommodation (Figure 2A.2). Upon reaching the inner cortex, the main direction of fungal growth shifts from radial (penetrating cell layers) to longitudinal (spreading intercellularly within the cortex). Short side branches from these intercellular spreading hyphae then penetrate the cortical cell through the PPA and branch dichotomously within the cell lumen to produce the highly branched arbuscules (Figure 2A.3-6). This strategy increases the contact surface between the host plant and the fungus (Smith & Read, 2008).

The plant cell undergoes significant reorganization in preparation for and during intracellular fungal accommodation. As the fungus proliferates within the cortical cell, the host plant's plasma membrane is invaginated but not penetrated, enveloping the fungal hyphae and all its branches. This forms the periarbuscular membrane (PAM), which is a specialized extension of the plant plasma membrane (Figure 2B). The PAM and the fungal plasma membrane delimit an interfacial zone, known as periarbuscular space, where nutrients and signals are exchanged (Cargill et al., 2025; Choi et al., 2018; Smith & Read, 2008).

The nutrient exchange across the PAM is bidirectional and reciprocal, forming the core of the mutualistic symbiosis. AMF acquire primarily phosphorus and nitrogen from the soil via extraradical mycelium and transfer it to the plant. AM-inducible phosphate and ammonium transporters, such as PT4 and AMT4, respectively, are critical for this process and are specifically localized at the PAM, near the fine branch domain of the arbuscule. The host plant supplies photosynthetically fixed carbon to the fungus, such as sugar and fatty acids.

This exchange is tightly regulated. Plant's nutritional status, particularly its phosphate levels, controls the establishment and maintenance of the symbiosis. Under phosphate starvation conditions, the release of SLs from plant roots is increased, which acts as a potent stimulant for fungal metabolism and hyphal branching, facilitating AM colonisation. Conversely, high levels of Pi can inhibit AM colonisation (Choi et al., 2018; Rui et al., 2022).

Arbuscules are ephemeral structures with a lifespan of only a few days. Their degeneration typically begins with the collapse of the fine branches, gradually progressing towards the trunk, accompanied by the retraction of fungal cytoplasm and the formation of septa to separate the degenerating from the living hyphae (Figure 2.7). This process is actively regulated by the plant, potentially as a defence mechanism against progressive fungal invasion or a response to an imbalance in nutrient exchange (Choi et al., 2018; Smith & Read, 2008).

Following the successful establishment of the symbiosis and the formation of these internal structures, the fungal mycelium continues to grow both within the roots and in the soil. As infection progresses and ages, thick-walled vesicles may be formed. Vesicles are important storage organs and play a significant role as propagules within root fragments, allowing the fungus to survive and potentially initiate new colonisation events from these fragments (Smith & Read, 2008).

AM fungi have historically been considered asexual because no morphologically identifiable sexual structures have been observed. Successful establishment and nourishment of the fungus by the plant are essential for asexual spore production. These spores can develop terminally or intercalary within a hypha, either singularly or in clusters, on sporogenic hyphae, primarily in the extraradical mycelium. Both patterns have been observed on the same mycelium in root organ cultures with *R. irregularis* (Cargill et al., 2025).

### 1.2.2 Signal transduction of CSSP in plants under AM symbiosis

The common symbiosis signalling pathway (CSSP) is a vital signalling cascade that orchestrates the establishment and maintenance of mutually beneficial interactions between plants and their microbial partners, such as AMF. Its activation is initiated by a precise molecular dialogue between both symbionts. As mentioned previously, host plant secretes SLs from its roots in order to attract AM fungal hyphae. Genes involved in SL biosynthesis are upregulated under phosphorus deficiency to promote mycorrhization (Ahmed et al., 2025; Ho-Plágaro & García-Garrido, 2022a).

The perception of SL by the fungus enhances the production of lipochitooligosaccharides and short-chain chitin oligomers, also known as Myc factors. These fungal signals trigger nuclear calcium spiking in plant root cells. (Ho-Plágaro & García-Garrido, 2022a). As shown in Figure 3, fungal Myc factors are primarily recognized by LysM receptor-like

kinases (RLKs). The SYMRK (symbiosis-receptor kinase), a plasma membrane-localised receptor-like kinase, is thought to act as a co-receptor in the recognition of fungal signals. It is essential for generating Myc-factor-induced calcium spiking. However, it is not known how the plasma membrane-localized SYMRK activates calcium spiking in the nucleus (Choi et al., 2018).

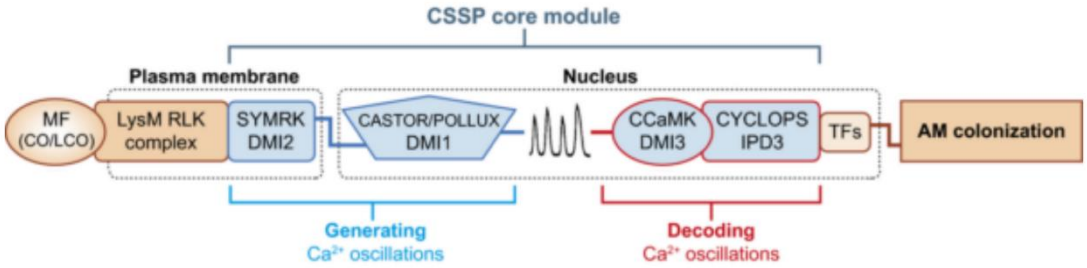


**Figure 3.** Schema illustrating the common symbiosis signalling pathway (CSSP) in AM symbiosis. The representation shows plant genes and secondary messengers required for the successful functioning of the conserved CSSP core module first found in *Lotus japonicus* (Lj) and *Medicago truncatula* (Mt). CSSP is activated by the perception of Myc factors (MF), namely short-chain chitin oligomers (CO) and lipochitooligosaccharides (LCO) by plasma membrane localized LysM-RLK receptors, most probably part of a larger complex including the leucine-rich repeat receptor-like kinase known as LjSYMRK/MtDMI2. Following signal transduction from the PM to the nucleus, nuclear membrane cation channels known as LjCASTOR/LjPOLLUX/MtDMI1 are then required for rapid $Ca^{2+}$ release and the initiation of nucleoplasmic $Ca^{2+}$ spiking. The subsequent decoding of the intranuclear $Ca^{2+}$ oscillatory response involves LjCCaMK/MtDMI3 and LjCYCLOPS/MtIPD3. Binding of $Ca^{2+}$ to the calcium and calmodulin-dependent kinase CCaMK leads to phosphorylation of the coiled-coil protein CYCLOPS. Finally, the activation of a downstream signalling cascade via GRAS transcription factors results in the synthesis of proteins required for the symbiosis, including the formation of the prepenetration apparatus. Adapted from Barker et al. (2017).

Located in the nuclear membrane, CASTOR and POLLUX are two cation channels required for rapid calcium release and the initiation of nucleoplasmic calcium spiking (Figure 3). This spiking activates the Calcium- and Calmodulin-dependent protein kinase (CCaMK), which phosphorylates the transcriptional activator CYCLOPS. CYCLOPS, in a complex with CCaMK and the protein DELLA, binds specific cis elements in gene promoters and activates the expression of key downstream genes, such as *RAM1* (Required for Arbuscular Mycorrhization 1; Figure 4). RAM1 is a GRAS-domain transcription factor (TF) essential for the formation of the PAM and for arbuscule branching, that is, for arbuscle development (Choi et al., 2018; Ho-Plágaro & García-Garrido, 2022a).

### 1.3 Cellular reprogramming in AM host plants

Arbuscule development needs to be accompanied by the cell expansion of cortex cells for the accommodation of arbuscules. At this regard, host plant cells undergo massive structural and functional modifications and members of the GRAS transcription factor family play an essential role in this transcriptional regulation of AM development.

### 1.3.1 GRAS transcription factors

GRAS family proteins are an important plant-specific family of transcription factors. They act as key regulators in the complex genetic reprogramming that orchestrates the AM symbiosis. The acronym GRAS is derived from the first three identified members: GIBBERELLIN-ACID INSENSITIVE (GAI), REPRESSOR of GA1 (RGA), and SCARECROW (SCR). All GRAS proteins share a conserved GRAS-domain in their C-terminal region. It consists of five distinct motifs: Leucine Heptad Repeat I (LHRI), VHIID, Leucine Heptad Repeat II (LHR II), PFYRE (or PYRE), and SAW. The LHRI motif is conserved across all GRAS proteins and contains nuclear localisation signals (NLSs), indicating their site of action is the nucleus (Ho-Plágaro & García-Garrido, 2022b; Jaiswal et al., 2022).

In contrast to the conserved C-terminus, the N-terminal region of GRAS proteins is highly variable and intrinsically disordered. This variability, which includes unique sequences and intrinsically disordered regions (IDRs), contributes to protein-protein interactions and gene-specific functions. Despite, the N-domain is highly conserved within the subfamily (Ho-Plágaro & García-Garrido, 2022b; Jaiswal et al., 2022).

Since the first subfamily division, the number of subfamilies has increased, with each plant species possessing GRAS genes included within 8 to 17 different subfamilies. Further research has been carried out and 19 subfamilies for the GRAS gene family have been currently identified, including DELLA and SCL3. Regarding the nomenclature of the GRAS subfamilies, the lack of consensus is still a complex issue (Neves et al., 2023).

GRAS proteins generally function as TFs or transcriptional regulators, which do not directly bind to DNA. They exert their functions mainly by forming homo- or heterodimers and interacting with other proteins to create regulatory complexes (Ho-Plágaro & García-Garrido, 2022b; Neves et al., 2023; Pimprikar & Gutjahr, 2018). Apart from their crucial role in AM symbiosis, GRAS proteins are implicated in a vast array of plant biological functions. Regarding plant and growth development, GRAS proteins are involved in shoot and root formation, radial root organization, microsporogenesis, fruit ripening, and seed germination. They also play a role in gibberellin (GA) signalling, where DELLA proteins act as key repressors. Additionally, GRAS proteins act in phytochrome signalling and light responses, and biotic and abiotic stress responses (Jaiswal et al., 2022; Neves et al., 2023).

### 1.3.2 Members of the GRAS family

In this chapter, the most relevant members of the GRAS protein family for this work are described.

**RAM1**

RAM1 is a crucial GRAS-type transcription factor in AM symbiosis. Its activity leads to transcriptional reprogramming of the host plant, enabling the physiological and morphological changes required for successful symbiosis. RAM1 is strongly and specifically induced upon root colonisation by AMF, and RAM1 promoter activity is spatially restricted to arbuscule-containing cells (Ho-Plágaro et al., 2019; Pimprikar & Gutjahr, 2018). Its transcription is primarily regulated by a CCaMK-CYCLOPS-DELLA complex. (Pimprikar & Gutjahr, 2018).

RAM1 acts as an early transcriptional switch to regulate downstream cascades (Figure 4) required for the transition from low-order to high-order fine branching of the arbuscule (Jaiswal et al., 2022). It also regulates the expression of genes involved in nutrient and lipid biosynthesis between the plant and the fungus by interacting with RAD1 and NSP2 (Figure 4). These include genes for AM-specific phosphate transporters (e.g., *PT4*), ammonium transporters (e.g., *AMT2* family members), and lipid biosynthesis genes (Ho-Plágaro & García-Garrido, 2022a; Pimprikar & Gutjahr, 2018).

**DELLA**

DELLA proteins are known for being repressors of gibberellin responses (Jaiswal et al., 2022). GA signalling is a fundamental hormonal pathway in plants that intricately controls various aspects of growth, development, and environmental responses. In the absence of active GA, DELLA proteins accumulate and repress GA responses, thereby inhibiting plant growth (Ito & Fukazawa, 2021).

DELLA proteins work in concert with other GRAS transcription factors, such as MYCORRHIZA INDUCED GRAS1 (MIG1), MIG2, and MIG3, and SCARECROW-LIKE3 (SCL3), to control root cortical cell size and accommodate arbuscules (Seemann et al., 2022). DELLA also plays a role in arbuscule degeneration, forming a transcriptional regulatory complex with NSP1 and MYB1 (Figure 4). This regulatory module enables the transcription of genes encoding proteins with hydrolytic activities such as proteases and chitinases associated with arbuscular degeneration. This suggests a dual role for

DELLA in both arbuscule formation and turnover, depending on the specific protein complexes it forms (Ho-Plágaro et al., 2019).

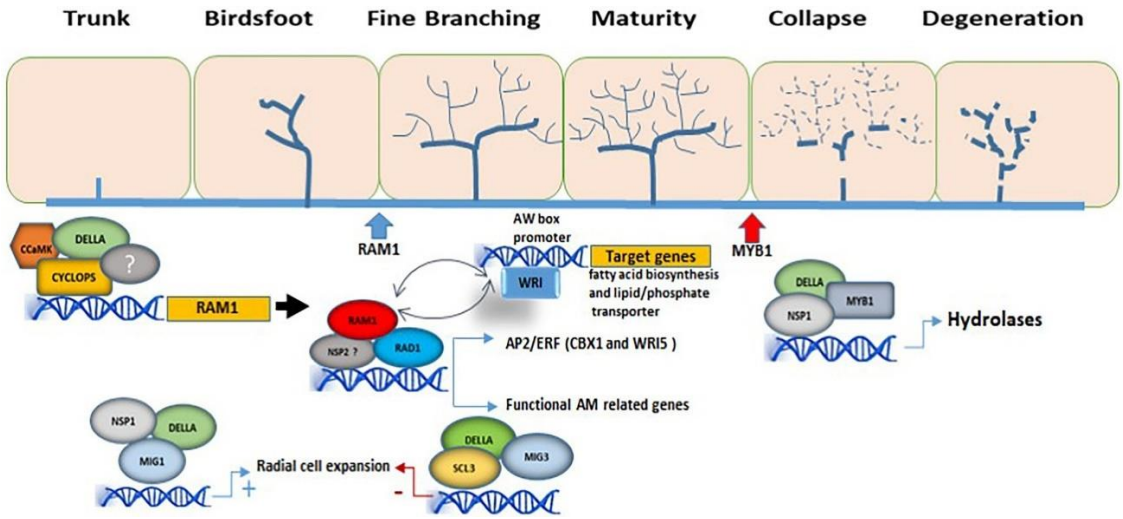


**Figure 4.** Involvement of GRAS TFs in the regulation of arbuscule formation. The DELLA/CYCLOPS/CCaMK complex regulates the expression of RAM1. In this manner, RAM1 is able to interact with several other GRAS-domain proteins such as RAD1, regulating the expression of genes involved in arbuscule development and functionality, as well as with TFs from the WRI family (CBX family in *L. japonicus,* harbouring an AP2/ERF domain), activating genes involved in lipid biosynthesis and in nutrient exchanges at the periarbuscular membrane. WRI and RAM1 regulate each other at the transcriptional level. The interaction of the GRAS-domain protein MIG1 with DELLA and NSP1 is necessary to regulate genes involved in the radial expansion of cortical cells for AM fungal accommodation, while SCL3, together with MIG3 and DELLA, counteracts the positive effect of MIG1 on cell expansion. MYB1 is required for the transcriptional regulation of genes involved in arbuscule degeneration (hydrolytic activity) and interacts with both DELLA proteins and the GRAS-domain protein NSP1. The different stages of arbuscule development are shown. The blue and red arrows mark the beginning of RAM1 activity and MYB1 activity, respectively. From Ho-Plágaro & García-Garrido **(2022b)**.

## MIG

MIG TFs belong to a novel clade of GRAS-domain proteins and are transcriptionally upregulated during mycorrhizal colonisation (Ho-Plágaro et al., 2019). MIG1 exhibits a mycorrhiza-specific expression pattern, being mainly confined to cortical cells containing arbuscules, even though in non-mycorrhizal roots, it is active in the central cylinder (Seemann et al., 2022). MIG2 and MIG3, while expressed more ubiquitously than MIG1 under non-symbiotic conditions, also show enhanced expression in cortical cells harbouring arbuscules during mycorrhization. The promoters of MIG genes contain the cis-regulatory element CTTC motif (Seemann et al., 2022). See chapter 1.3.4 for a better understanding of CTTC motif.

MIG proteins are key regulators of cortical cell size. MIG1 and MIG2 act as positive regulators of cortical cell expansion, whereas MIG3 acts as a negative regulator interacting with SCL3. All MIG proteins are able to interact with DELLA proteins (Ho-Plágaro & García-Garrido, 2022b; Seemann et al., 2022).

### 1.3.3 SlGRAS18 transcription factor

SlGRAS18 TF has been characterised as an ortholog of *Arabidopsis thaliana* AtSCL3, in *Solanum lycopersicum* (tomato), belonging to the SCL3 subfamily of GRAS proteins (Ho-Plágaro et al., 2019). SlGRAS18 does not contain any known direct DNA binding domains. Instead, it is thought to function as a transcriptional regulator or co-factor, operating within transcriptional complexes by interacting with other transcription factors that do possess DNA-binding domains (Avilés-Cárdenas et al., 2024). SlGRAS18 has been shown to interact strongly with itself, suggesting the formation of homodimers (Avilés-Cárdenas et al., 2024). This dimerization may play an important role in its functionality.

SlGRAS18 acts as a negative regulator of arbuscule formation. Silencing of SlGRAS18 positively impacts arbuscule development, leading to an increase in the number of large and well-developed arbuscules at late stages of colonisation. This silencing also leads to an improvement in symbiotic efficiency, measured by enhanced physiological traits such as flowering and fruit development, and a discernible pattern of mineral nutrient redistribution in leaves (Avilés-Cárdenas et al., 2024). Like its ortholog AtSCL3 in the non-host for AM symbiosis *A. thaliana*, SlGRAS18 is hypothesized to be involved in controlling the action of gibberellins during AM development. AtSCL3 functions as a positive regulator of GA signalling by antagonizing DELLA proteins (Zhang et al., 2011).

Seemann et al. (2022) proposes a model in *M. truncatula* in which the regulation of cortical cell size during AM symbiosis is mediated by the interaction between MIG, SCL3 and DELLA proteins (Figure 4). The mechanism is described as a “tug-of-war”. In this model, MIG3 interacts with SCL3, primarily in the nucleus. The MIG3-SCL3 complex modulates DELLA activity to restrain cortical cell growth and expansion, which is essential for arbuscule development. This complex antagonizes the function of the MIG1-DELLA complex, which promotes cortical cell expansion to accommodate the developing arbuscule. Avilés-Cárdenas et al. (2024) found that not only MIG3 interacts with SlGRAS18, but MIG3 also induces SlGRAS18 expression under mycorrhizal conditions.

SlGRAS18 is not only abundant in roots, but it is also expressed in developing fruit, indicating that this TF has other roles outside arbuscular mycorrhization. As an SCL3 group member, SlGRAS18 is hypothesized to function as a positive regulator of

gibberellin signalling and to be involved in mediating GA-promoted cell elongation during root development (Avilés-Cárdenas et al., 2024; Ho-Plágaro et al., 2019).

### 1.3.4 CTTC mycorrhizal promoter motif

The CTTC motif, also known as mycorrhiza transcription factor binding sequence (MYCS), is a cis-regulatory element involved in the transcriptional activation of genes in plants, particularly those related to AM symbiosis. The CTTC motif has been identified in the promoter of several genes expressed in arbuscule-containing cells (Pimprikar & Gutjahr, 2018; Seemann et al., 2022).

The CTTC motif is typically found close to the ATG start codon, in the promoter. Its consensus sequence stands for [T/C][T/G][T/A]CTTGTT[C/T/G][T/C], according to Pimprikar & Gutjahr (2018). In this work, four CTTC motifs were identified upstream of the SlGRAS18 start codon ATG, which are shown in Figure 5. One of them, the 4$^{th}$ CTTC motif, was found to belong to the 5'-UTR region of *SlGRAS18*.


**Figure 5.** Graphical representation of *SlGRAS18* gene and an approximately 700 bp long fragment of its promoter, indicating the positions of four CTTC motifs. CTTC motifs are a cis-regulatory element found in the promoters of genes induced upon mycorrhization. 2$^{nd}$ CTTC motif: from -386 to -376 bp; 1$^{st}$ CTTC motif: from -302 to -292 bp, 3$^{rd}$ CTTC motif: from -223 to -213 bp, 4$^{th}$ motif: from -66 to -56 bp. The latter belongs to the 5'-UTR region of *SlGRAS18*, which extends from -182 to -1 bp. All four motifs are located in the + strand.

## 1.4 Model organisms

### 1.4.1 *Solanum lycopersicum*

Tomato (*S. lycopersicum*) is widely used as a model organism due to a combination of its agricultural significance, favourable genetic characteristics, and the availability of advanced research tools. It is an economically important crop grown worldwide. This vegetable accounts for 10.6% of the EU's total fresh vegetable cultivation area, yielding 15.4 million tonnes of harvested production in 2022 (Eurostat, 2024). This makes research into this species highly relevant for improving agricultural practices and crop yields. Additionally, tomato is also susceptible to various pests and diseases, making studies on beneficial rhizosphere microorganisms such as AMF particularly valuable (Ho-Plágaro et al., 2018).

This species possesses a relatively compact genome of approximately 950 Mb (Ho-Plágaro et al., 2018), and a marker-saturated genetic linkage map and an annotated genome sequence are available. Unlike potato, which is tetraploid, tomato is diploid making genetic editing more straightforward, and seeds can be easily obtained (Ho-Plágaro et al., 2018). Furthermore, stable transformations with *Agrobacterium tumefaciens* are easier to perform in tomato than in *M. truncatula*, another crop used for research in AM symbiosis. Tomato benefits from highly efficient transformation protocols, including a rapid and reliable *Agrobacterium rhizogenes*-mediated transformation method described by Ho-Plágaro et al. (2018), which was used in this work.

### 1.4.2 *Rhizophagus irregularis*

*R. irregularis* is a widely used model fungus for AM symbiosis. It can be cultivated in monoaxenic cultures with a host, such as carrot roots, which provides a controlled environment for experiments (St-Arnaud et al., 1996). This AMF is a generalist symbiont that reliably forms mycorrhizal associations with diverse plant hosts and is highly efficient at spore production and symbiosis establishment, enabling reproducible colonisation of roots. Additionally, its genome has been fully sequenced and annotated.

## 1.5 *Agrobacterium rhizogenes*-mediated transformation

*A. rhizogenes*, now renamed as *Rhizobium rhizogenes* (Young et al., 2001), is a gram-negative soil bacterium that is a close relative of *A. tumefaciens*, the bacterium responsible for crown gall disease. *A. rhizogenes* is the causative agent of hairy root disease in plants, which is characterized by the overgrowth of adventitious roots at the infection site (Mauro & Bettini, 2021).

The infection process of *A. rhizogenes* involves a sophisticated mechanism of horizontal gene transfer. The bacterium typically thrives near plant roots and enters through wounded sites, which release phenolic compounds such as acetosyringone. These phenolic compounds attract *A. rhizogenes* through chemotactic movement and induce the expression of *vir* (virulence) genes. These genes coordinate the processing and transference of T-DNA (transfer DNA) from the *A. rhizogenes* root-inducing (Ri) plasmid to the host plant's cell. This T-DNA contains a set of genes called *rol* (root locus) genes (A, B, C, and D), which alter hormone perception by the plant and are primarily responsible for inducing the hairy root syndrome, leading to the formation of highly

branched roots at the infection site. The T-DNA also encodes one or more enzymes for the biosynthesis of phytohormones and opines, which accumulate in hairy roots and provide a nutrient source that Agrobacteria are capable of utilizing as carbon and nitrogen sources (Bagal et al., 2023; Goralogia et al., 2025; Mauro & Bettini, 2021).

*A. rhizogenes* strains can be "disarmed" by the removal of opine biosynthetic genes and *rol* genes present in T-DNA, which can be replaced by DNA sequences of interest, such as reporter genes. Disarmed strains can be biotechnologically used to generate composite plants, which consist of wild-type shoots with genetically transformed roots. A binary system can be used in *A. rhizogenes*-mediated transformation, in which the Ri plasmid contains the *vir* genes, and another binary vector carries the T-DNA sequence with the gene of interest. The T-DNA on the binary vector is flanked by specific border sequences (LB and RB) that are recognized by the *vir* machinery on the Ri plasmid (Goralogia et al., 2025).

This method offers a fast and reliable alternative to stable transformation, particularly for research focused on root biology. Composite plants can be obtained within 10 weeks and, therefore, is by far faster than a stable transformation of the hole plant with *A. tumefaciens*, which takes around 4-6 months.

## 2. SIGNIFICANCE OF THE STUDY

AMF significantly improve the host plant's uptake of mineral nutrients and water, and promote plant tolerance to various abiotic stresses such as drought, by changing root morphology, salinity, by maintaining proper ion homeostasis, and heavy metal toxicity, by increasing phosphate content and promoting the growth dilution effect. They also counteract oxidative stress by increasing the activity of antioxidant enzymes and reducing reactive oxygen species (Bennett & Groten, 2022; Shi et al., 2023). Regarding to biotic stresses, AM symbiosis can prime host plant's immunity, leading to more efficient immune response against pathogens and herbivores. AMF can also alter plant volatile compounds and root exudates, providing direct and indirect defences against herbivores and minimizing the invasion of root-knot nematodes and parasitic plants (Bennett & Groten, 2022; Shi et al., 2023).

Mycorrhizal networks, formed by interconnected AM fungal hyphae, allow the transfer of nutrients and signals between connected plants. They can also facilitate the

mycorrhization and nourishing of neighbour seedlings. AM symbiosis enhances the diversity of plant communities and promotes soil formation and increased macroaggregate stability. Furthermore, these mycorrhizal networks represent a key entry point for carbon absorption in the soil and can influence other soil microbes in the rhizosphere (Cargill et al., 2025; Shi et al., 2023). AM symbiosis holds significant potential for improving agricultural sustainability and crop production as biofertilisers and bioprotectors.

However, the regulatory mechanisms controlling this interaction remain only partly understood. In particular, the role of the CTTC motif in the regulation of mycorrhiza-induced TFs such as SlGRAS18 has not been fully characterized. This study contributes to filling this gap, even though more research needs to be done. Beyond advancing basic knowledge, the findings may have further practical implications in the development of crops with enhanced mycorrhization, which could improve plant health and production, and reduce dependence on chemical inputs in agriculture.

## 3. HYPOTHESIS OF THE WORK AND OBJECTIVES

This work is based on the hypothesis that a 240 bp fragment located upstream of the ATG start codon from *SlGRAS18*, which includes the 4$^{th}$ CTTC motif, is sufficient to confer AM-induced expression in arbuscule-containing cells of mycorrhizal *S. lycopersicum* cv. Moneymaker.

The organic aim of this project was to enhance mycorrhization in tomato plants in order to promote plant health and resistance to pathogens, thereby leading to more vigorous and productive crop plants. To meet the target, research was focused on the regulation of the gene *SlGRAS18*, contributing to identify which CTTC motif upstream of its start codon is required for the induction of its own expression under arbuscular mycorrhizal conditions.

**This goal aligns with the Farm to Fork strategy of the European Green Deal, which promotes the reduction of chemical inputs in agriculture. The use of AMF contributes to key goals of the EU carbon farming strategy by enhancing soil health, increasing biodiversity, and improving plant resilience to abiotic stress associated with climate change.**

Consequently, the specific objective of this work was to conduct an *A. rhizogenes*-mediated composite transformation of *S. lycopersicum* cv. Moneymaker for a promoter truncation analysis with GUS reporter assay, using either a 240 bp or a 700 bp fragment upstream of the *SlGRAS18* start codon.

# 4. MATERIALS AND METHODS

## 4.1 Biological material

*S. lycopersicum* cv. Moneymaker seeds were obtained from Horti Tops™ (Enkhuizen, The Netherlands). Moneymaker is a widely used cultivar in studies involving *Agrobacterium*-mediated transformation and symbiotic interactions. It has a well-annotated genome and allows for reproducibility across different experiments. This cultivar has been used in studies such as Ho-Plágaro et al. (2019) and Avilés-Cárdenas et al. (2024).

The strain *A. rhizogenes* ARquaI from Quandt (1993) was used for the composite transformation. It is a derivative of the strain R1000, which at the same time derives from the wild-type strain A4T. ARquaI is a disarmed strain commonly used for creating composite plants with transgenic roots and wild-type shoots.

For mycorrhizal experimental groups, the monoaxenic *R. irregularis* DAOM 181602 from Schenck & Smith (1982) was used for mycorrhization. This strain is a wild isolate, well-characterized, and its widespread use in mycorrhizal research facilitates the comparison of results across different studies.

## 4.1 CTTC motif identification

A manual search for CTTC motifs was performed within the promoter and 5'-UTR region of *SlGRAS18*, using the sequence available at Ensembl Plants (https://plants.ensembl.org/). The accession number for *SlGRAS18* is Solyc01g008910. A region of 2 kb upstream of the start codon was screened, including the annotated 5'-UTR region, based on the consensus CTTC sequence [T/C][T/G][T/A]CTTGTT[C/T/G][T/C], according to Pimprikar & Gutjahr (2018).

The 4$^{th}$ CTTC motif was selected for analysis in this work, since it is the closest to the ATG start codon, and it is supposed to have more influence on *SlGRAS18* expression.

### 4.2 Germination of tomato seedlings for *A. rhizogenes* transformation

Figure 6 shows a schematic view of the whole GUS reporter assay for truncation promoter analysis, including the generation of composite plants, and WGA-FITC counterstaining for fungal visualisation.

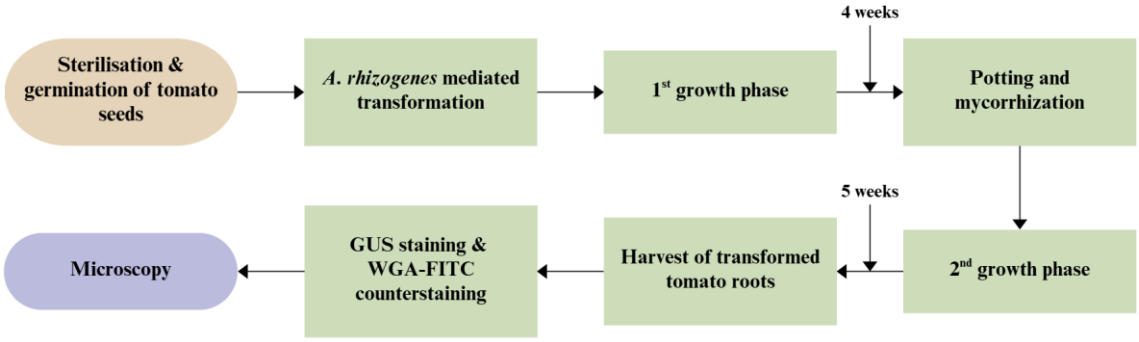


**Figure 6.** Flowchart of the GUS reporter assay performed in this study. The schematic view comprises the generation of *A. rhizogenes*-mediated composite tomato plants for GUS reporter assay of the 240 bp and 700 bp *SlGRAS18* promoter fragments, as well as WGA-FITC counterstaining for further visualisation of fungal structures.

Seed surface sterilization (n=229) was performed by immersing seeds in 70% (v/v) ethanol for 1 minute followed by three washes with sterile distilled water. Afterwards, seeds were soaked in a sodium hypochlorite solution (28 g/L NaClO in water) under continuous agitation for 10 minutes and rinsed three more times with distilled water. Subsequently, seeds were distributed onto water agar plates (9 g/L agar in water; agar from Carl Roth GmbH & Co., Karlsruhe, Germany; cat. no. 5210.2) and kept overnight at 4 ºC in the dark for cold stratification. Plates were then incubated at 28 ºC in the dark for three days to allow root emergence (Figure 7a).

Afterwards, the 192 germinated tomato seedlings were transferred onto 90 mm Petri dishes (Figure 7b) containing inclined 0.5x MS agar medium without sucrose (15 g/L agar; see Annex 2) and incubated for 4 days under a 16 h light (25 ºC) /8 h dark (20 ºC) photoperiod for cotyledon emergence. The MS medium, originally developed by Murashige & Skoog (1962) for *in vitro* culture of plant tissues, was used here with slight modifications in its concentrations. It is commonly used due to its high concentration in macronutrients, particularly nitrogen, which support rapid cell division and shoot proliferation. In this case, 0.5x MS agar medium must not contain a carbon source, as it is the medium where the transformation is going to take place and bacteria should grow towards the seedling to perform the transformation, rather than throughout the medium.

### 4.3 Tomato seedlings transformation with *A. rhizogenes*

Germination and transformation of tomato seedlings with *A. rhizogenes* ARquaI were performed according to the protocol of Ho-Plágaro et al. (2018), with some modifications, which corresponds to the standard procedure in the laboratory. Three different binary plasmids were used separately:

- #4551: 240 bp *SlGRAS18* promoter::pGFPGUS-RedRoot. The symbol '::' indicates a transcriptional fusion between a promoter and a reporter gene. This construct contains, in the T-DNA region, the *GFP* (green fluorescent protein) and *GUS* (β-glucuronidase) reporter genes under the control of a 240 bp fragment located upstream of the *SlGRAS18* start codon ATG. Additionally, the T-DNA region contains the *DsRed* gene, a visual marker protein with red fluorescence, under the control of the constitutive promoter *tNOS*.
- #4552: 700 bp *SlGRAS18* promoter::pGFPGUS-RedRoot. This construct is similar to #4551 but it contains a 700 bp fragment upstream of the *SlGRAS18* ATG sequence, which comprises the four identified CTTC motifs.
- #2469: Empty vector; pPGFPGUS-RedRoot. This vector lacks any promoter insert and was used as a transformation and negative control.

All three constructs had been previously generated and transformed into *A. rhizogenes* in Natalia Requena's laboratory, and subsequently stored at −80 °C.

For the Ri-transformation (*A. rhizogenes*-mediated transformation), the radicle and lower part of the hypocotyl of each tomato seedling (192 in total) were removed, leaving approximately 1 cm of the apical part of the hypocotyl. The remaining stem was wounded by scratching it with a syringe coated with *A. rhizogenes* ARqua1 containing the corresponding plasmid for each experimental group. Subsequently, the syringe was punctured into the 0.5x MS medium to deposit the *A. rhizogenes* cells next to the stem (Figure 7c). The wounded seedlings were kept on the same plate for 1 week under a 16 h light (25 ºC) /8 h dark (20 ºC) photoperiod. For each experimental group, 64 seedling transformations were performed.

After that time, the emerging roots were excised with a sterile scalpel, since the first appearing roots are typically non-transformed. Seedlings were transferred to new Petri dishes containing 0.5x MS agar medium without sucrose nor vitamins (15 g/L agar, see

Annex 2), to promote new root development, likely due to a mild stress response (Ho-Plágaro et al., 2018). They were incubated under the same conditions for 3 more weeks.

After the 4-week growth phase (Figure 7d), new roots were checked visually under green light using the SteREO Lumivar V12 binocular microscope equipped with AxioCam HRc (Zeiss, Oberkochen, Germany) to verify successful transformation. Positive root transformants were recognisable by red fluorescence of DsRed and were marked (Figure 7e), whereas non-transformed roots were sterilely excised with a scalpel. DsRed protein has an excitation peak at a wavelength of 558 nm (green light) and an emission peak at 583 nm (red light). See Table 1 for the total number of successfully transformed seedlings.

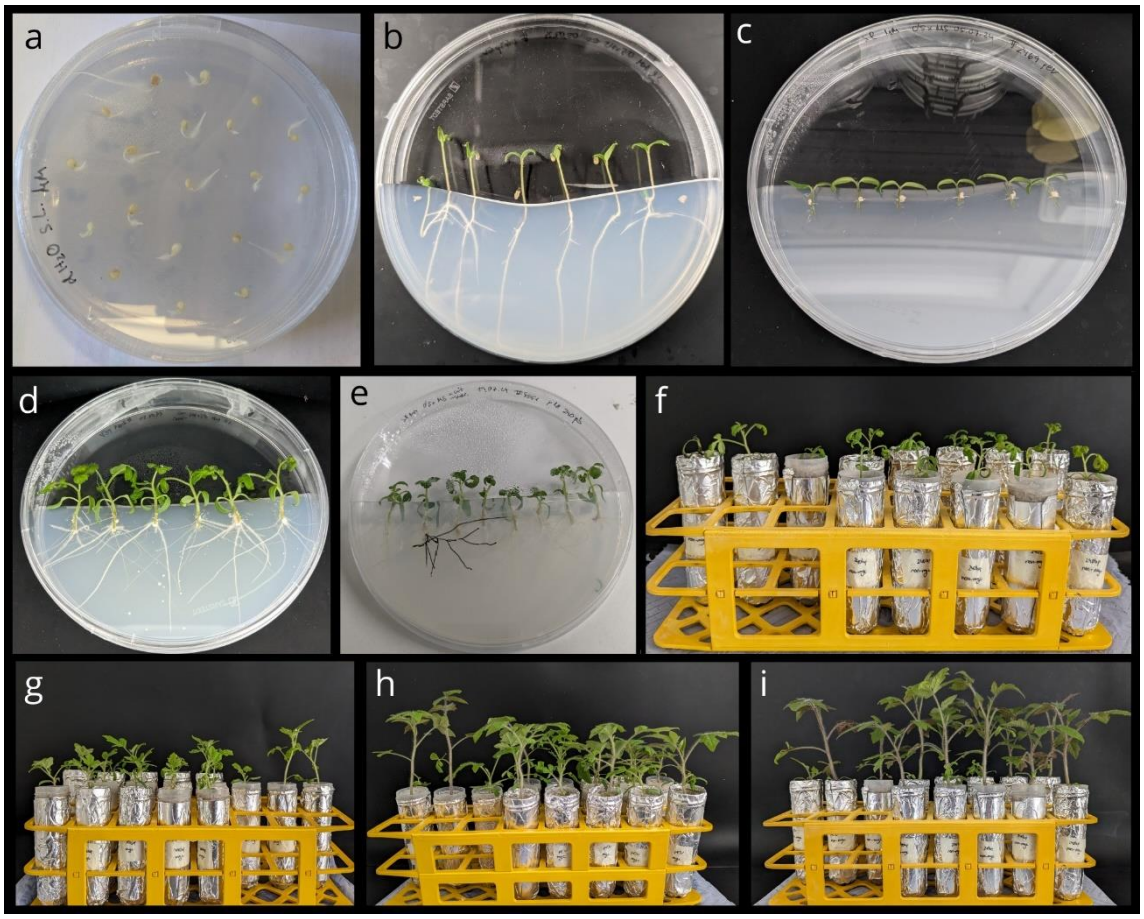


**Figure 7.** Workflow of *A. rhizogenes*-mediated transformation and potting of tomato plants. (a) Root emergence from *S. lycopersicum* cv. Moneymaker on water agar medium after 4 days of incubation. (b) Tomato seedlings 4 days after transfer onto 90 mm Petri dishes containing inclined 0.5x MS medium without sucrose. (c) Tomato seedlings after *A. rhizogenes*-mediated transformation. Bacteria can be seen as a small yellow/beige dot beside the stem of each seedling. (d) Tomato seedlings 27 days post-transformation. (e) Transformed roots marked in black after using a fluorescent binocular microscope to visualize DsRed expression. This took place on the potting day, one month after germination, and only seedlings with transformed roots were potted. (f-i) Tomato plants at 3 (f), 9 (g), 16 (h), and 22 (i) days after potting.

### 4.4 Potting and harvest

The transformed composite plants were potted under non-sterile conditions into sterilized 50 mL Falcon tubes filled with a previously washed and autoclaved fine and coarse sand mixture (3:1), and incubated for 5 weeks under a 16 h light (25 ºC) /8 h dark (20 ºC) photoperiod (Figure 7f). Falcon tubes had been perforated with 4 holes at the bottom to allow water drainage. They were wrapped with aluminium foil to protect the roots from light and filled with some previously dry-sterilized stones. Throughout the 5-week period (Figure 7g-i), tomato composite plants were watered with 5 mL of autoclaved distilled water and fertilized with 5 mL of 0.5x Hoagland solution (15 mM N and 20 μM Pi; see Annex 2) every Monday, Wednesday, and Friday until harvest. The Hoagland solution is a fertiliser commonly used in hydroponics and plant physiology experiments. The composition used in this project is based on Javot et al. (2011). Since it is half-strength, it provides phosphate-limiting conditions, which enhance mycorrhization. To ensure a constant humidity level, the potted plants were covered with a small plastic bag for the first 16 days.

After 4 weeks from potting, composite plants were harvested. Plants were carefully removed from the sand mixture and rinsed with distilled water (see Figure S 2 in Annex 3 for an additional image). Fresh weight of the shoot was determined separately using a precision balance. The shoots were subsequently discarded. Roots were again checked under green light with the SteREO Lumivar V12 binocular, and untransformed roots were discarded.

### 4.5 Propagation of *R. irregularis* and mycorrhization

The fungus *R. irregularis* DAOM 181602 (Schenck & Smith, 1982) was cultivated in monoaxenic dual culture with *A. rhizogenes*-transformed *Daucus carota* (carrot) roots on Minimal (M) medium (see Annex 2) at 28 °C in the dark, following the system proposed by St-Arnaud et al. (1996) with modifications. M medium, described by Bécard & Fortin (1988), is widely used for *in vitro* cultivation of AMF. As *R. irregularis* requires colonisation of a host plant to complete its life cycle, it was propagated in *A. rhizogenes*-transformed carrot roots, which continuously grow due to the production of endogenous phytohormones. Every 6-8 weeks, 3-4 root segments were transferred to fresh medium for further propagation (see Figure S 3 in Annex 3 for additional images).

For mycorrhization of tomato plants during potting, 10 plates containing mycorrhizal *D. carota* roots were used for the mycorrhization of tomato plants during potting. Prior to use, the plates were inspected for contamination and sufficient spore production. Roots were separated from M medium and soaked in distilled water, which was evenly mixed with the sand substrate used for potting. Non-mycorrhizal plants did not receive any additional treatment. Table 1 shows the final number of potted composite plants of each experimental group.

**Table 1.** Number of successfully transformed seedlings, as well as mycorrhizal and non-mycorrhizal potted plants. The total number of each experimental group corresponds to the number of successfully transformed seedlings.

| Construct | Mycorrhizal | Non-mycorrhizal | Total |
|---|---|---|---|
| Empty vector (#2469) | 5 | 4 | 9 |
| p240 bp (#4551) | 7 | 5 | 12 |
| p700 bp (#4552) | 5 | 4 | 9 |

### 4.6 GUS staining of the roots

To analyse the promoter activity of a gene, the corresponding promoter is cloned upstream of the β-glucuronidase (GUS) reporter gene from *Escherichia coli*. The promoter activity is visualised by so-called GUS staining, in which X-Gluc (5-bromo-4-chloro-3-indolyl-ß-D-glucuronide) sodium salt is used as a substrate, that hydrolysed by the expressed β-glucuronidase is converted into the blue 5,5'-dibromo-4,4'-dichloro-indigo dye. In this sense, staining is higher with strong promoter activity and lower with weak promoter activity (Jefferson et al., 1987).

Transformed roots were cut into 2 cm-long root fragments and transferred into Eppendorf tubes containing 1 mL of fixation buffer (50 mM sodium phosphate, pH 7.0; 1 mM $Na_2EDTA$; 0.37% (v/v) formaldehyde) for 30 minutes. Afterwards, the fixation buffer was removed, and roots were rinsed three times with 1 mL of washing buffer (50 mM sodium phosphate, pH 7.0; 1 mM $Na_2EDTA$). After the final rinse, 1 mL of staining buffer (50 mM sodium phosphate, pH 7.0; 1 mM $Na_2EDTA$; 1 mM X-Gluc from a 0.1 M stock solution in DMF; X-Gluc from Apollo Scientific Ltd, Bredbury, United Kingdom; cat. no. BIMB1121) was added, and roots were incubated overnight at 37 ºC. The next day, roots were rinsed again 3 times with 1 mL of washing buffer and incubated for 3 hours in 50% (v/v) ethanol.

### 4.7 WGA-FITC counterstaining of the roots

Wheat Germ Agglutinin conjugated to Fluorescein Isothiocyanate (WGA-FITC) is a lectin-fluorophore conjugate commonly used for the specific labelling of fungal cell walls within plant tissues. The excitation maximum of FITC is at 492 nm, and the emission at 520 nm.

Roots were cleared in 10% (w/v) KOH at 90 ºC for 30 minutes. After clearing, roots were washed 3 times with 1x PBS buffer (10 mM $Na_2HPO_4$; 1.8 mM KH2PO4; 0.14 M NaCl; and 2.7 mM KCl dissolved in dH2O, pH 7.3) containing 0.02% (w/v) Tween® 20 (AppliChem GmbH, Darmstadt, Germany; cat. no. A1389.0500) and acidified with 1% HCl (v/v) for 5 minutes. They were subsequently washed 3 times with distilled water, followed by a wash with PBS buffer containing 0.02% (w/v) Tween® 20. Roots were then incubated overnight at 4 ºC in WGA-FITC solution (5 µg/mL). Afterwards, they were washed 3 times with 1x PBS buffer with 0.02% (w/v) Tween® 20 and stored in the dark at 4 ºC until further microscopy analysis.

### 4.8 Microscopy analysis of GUS reporter assay

For the microscopy analysis of *S. lycopersicum* cv. Moneymaker transformed roots, a Leica TCS SP5 confocal laser scanning microscope (Leica Microsystems GmbH, Wetzlar, Germany) was used. Fungal structures counterstained with WGA-FITC were imaged by exciting the fluorophore with an argon laser at 488 nm. Fluorescein emission was detected between 505 and 525 nm. Promoter activity was visualised using the Leica DFC295 colour camera attached to the confocal microscope by capturing the blue GUS staining.

### 4.9 Statistical analysis

Data were processed statistically using PSPP (GNU PSPP version 2.0.0) and were represented graphically using Excel. Prior to parametric testing, the Shapiro–Wilk test was used to assess the normality of the data distribution within each group, and Levene's test was applied to verify the homogeneity of variances across groups. As both assumptions were met ($p > 0.05$), parametric tests were considered appropriate.

A two-way analysis of variance (ANOVA) was conducted to examine the effects the promoter fragment used (empty vector, pEV; 240 bp *SlGRAS18* promoter fragment, p240; and 700 bp *SlGRAS18* promoter fragment, p700) and mycorrhizal condition (mycorrhizal,

M; non-mycorrhizal, NM), which are two independent factors, as well as their interaction, on tomato shoot fresh weight. Since no significant main effects or interactions were observed ($p > 0.05$), a complementary one-way ANOVA was carried out, treating the six treatment combinations (pEV-M, pEV-NM, p240-M, p240-NM, p700-M, and p700-NM) as independent groups. This was followed by Fisher's Least Significant Difference (LSD) post-hoc test to detect potential pairwise differences between treatments.

# 5. RESULTS AND DISCUSSION

## 5.1 Localisation of CTTC motifs

By performing a manual search for CTTC motifs within the promoter and 5'-UTR region of *SlGRAS18*, four CTTC motifs were determined (Figure 5), one of them belonging to the 5'-UTR region. By contrast, Avilés-Cárdenas et al. (2024) did not localise any CTTC motif upstream of the start codon of *SlGRAS18*. This difference could lie in the fact that, in our work, a single nucleotide mismatch from the consensus sequence [T/C][T/G][T/A]CTTGTT[C/T/G][T/C] was allowed, while maybe Avilés-Cárdenas et al. (2024) did not allow any.

CTTC motifs have been found upstream of the start codon from *SCL3*, an ortholog of *SlGRAS18* in *M. truncatula* (Seemann et al., 2022), and from *MIG* genes (belonging also to the GRAS TF family), also in *M. truncatula* (Heck et al., 2016). This motif has been identified in the promoter of several genes induced upon arbuscular mycorrhization, such as the PAM-localised phosphate transporter *PT4* (Paries et al., 2025; Pimprikar & Gutjahr, 2018; Xue et al., 2018).

Since motifs located upstream close to the ATG have the highest probability of being essential for the induction of the subsequent gene, promoter truncation analysis is used in this work to shorten the promoter of *SlGRAS18* in order to elucidate if the 4$^{th}$ CTTC motif is sufficient to induce the expression of the gene under mycorrhizal conditions, using a GUS reporter system.

## 5.2 Effects of GUS reporter assay in shoot weight

Shoot fresh weight was measured after harvest. A slight increase in weight was observed in the mycorrhizal 240 bp *SlGRAS18* promoter fragment group, although it was not statistically significant. No significant differences in shoot fresh weight were observed

between constructs (empty vector, 240 bp promoter fragment, and 700 bp promoter fragment) or mycorrhizal conditions (mycorrhizal and non-mycorrhizal), nor was there a significant interaction between these two factors, as determined by two-way ANOVA ($p > 0.05$). Consequently, one-way ANOVA was also performed on the six treatment combinations (promoter fragment used × mycorrhizal condition), followed by Fisher's LSD post hoc test. However, no statistically significant differences were found between any of the groups.

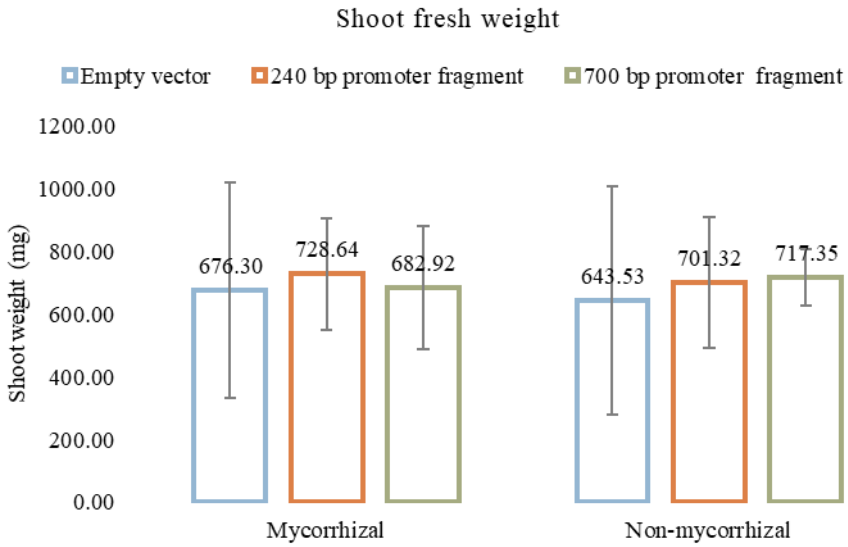


**Figure 8.** Bar plot of shoot fresh weight of transformed tomato plants under different promoter fragments (empty vector, 240 bp *SlGRAS18* promoter fragment, and 700 bp *SlGRAS18* promoter fragment) and mycorrhizal condition (mycorrhizal, non-mycorrhizal). Bars represent the mean ± standard deviation in whiskers (the number of samples of each group can be found on Table 1). The Shapiro–Wilk test was used to test for normal distribution, and Levene's test was applied to verify the homogeneity of variances across groups. No statistically significant differences were observed between treatments based on two-way and one-way ANOVA analyses followed by post-hoc Fisher's LSD ($p > 0.05$).

These results suggest that the expression of β-glucuronidase and the mycorrhizal treatments did not significantly influence shoot fresh weight under the tested conditions (Figure 8; see Annex 4 for statistical details). However, it must be taken into account that, since plants were Ri-transformed, the shoot remained wild-type. Additionally, it is important to note that the aim of this experiment was to test whether the 240 bp promoter fragment upstream of the *SlGRAS18* start codon was sufficient to induce its expression. Therefore, the focus was more on qualitative and localized gene expression, rather than quantitative traits such as fresh shoot weight. A whole-plant stable transformation would be required in order to evaluate parameters such as biomass, production and overall plant health.

### 5.3 Germination and transformation efficiencies

The germination efficiency was of 83.84%, leading to 192 plantlets able for the composite transformation. Lower percentage was obtained in the transformation at week 4, which was of 15.63%, whereas the survival rate of transformed plantlets was of 100%. A lower survival rate (about 90%) was observed in Ho-Plágaro et al. (2018). Instead of using Petri dishes with 0.5x MS medium at 1.5% agar, Ho-Plágaro et al. (2018) used their "sandwich" method, consisting of placing the hypocotyl of the plantlet between two filter papers on the MS medium.

The higher survival rate might be attributed to the use of agar-solidified medium that provides more stable physical support and possibly reduces mechanical stress on hypocotyl and emerging roots. It suggests that the standard methodology in the laboratory could be a reliable alternative for future experiments, being simpler and easier to implement than the original from Ho-Plágaro et al. (2018), even though the transformation efficiency should be increased.

A similar procedure to the one used in this work was studied by Tóth et al. (2022), obtaining a transformation efficiency of 90% 4 weeks after inoculation, although a more plant-individualised methodology was applied. Another variation of this work was the puncture of the hypocotyl with a tungsten needle dipped in bacterial mass as the infection method. Tóth et al. (2022) suggest that the tungsten needle might be effective since, due to its thin and smooth surface, it was able to cause minimal damage. A possible improvement would be a combination of both the standard procedure used in this work and the use of the tungsten needle puncture suggested by Tóth et al. (2022), in order to obtain a simple but efficient method.

### 5.4 Results of truncation analysis with GUS reporter assay

The activity of the different promoter and 5'-UTR region fragments from *SlGRAS18* was analysed. A 240 bp or 700 bp region upstream of *SlGRAS18* was fused to a GUS reporter construct, composite tomato plants were generated, and transgenic roots were checked for the presence of the blue dye corresponding to GUS activity. The 240 bp fragment contained the 4$^{th}$ CTTC motif, the closest to the start codon, hypothesised to be sufficient for gene induction, and the 700 bp fragment possessed all four CTTC motifs. Young lateral roots were preferred for microscopy, since they are more likely to be mycorrhizal

as they possess less secondary growth. The analysis was performed in mycorrhizal and non-mycorrhizal conditions. Results are shown in Figure 9.

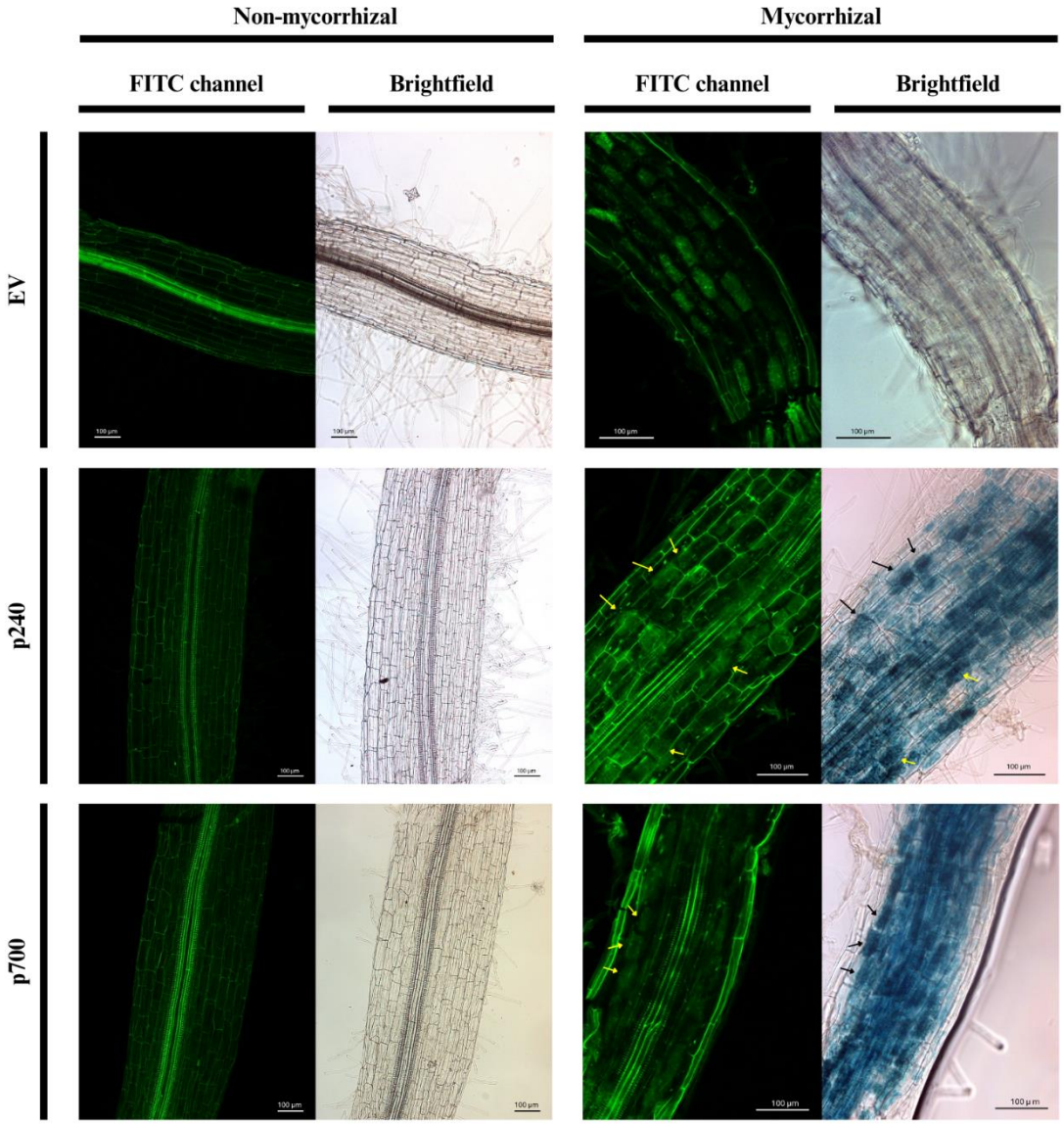


**Figure 9**. Truncation analysis of the *SlGRAS18* promoter activity in *A. rhizogenes*-transformed *S. lycopersicum* roots after GUS staining and WGA-FITC counterstaining. GUS activity in transformed roots expressing pGFPGUS-RedRoot fused to either a 240 bp (**p240**) or a 700 bp (**p700**) fragment upstream of ATG start codon from *SlGRAS18*, or without promoter sequence as a control empty vector (**EV**), was assessed after 4 weeks of inoculation with *R. irregularis*. WGA-FITC was imaged through the **FITC channel**, showing fungal structures, and GUS staining was imaged through the **brightfield channel**, both using a Leica TCS SP5 confocal laser scanning microscope. For every experimental group, the same root fragment is shown for both the FITC and brightfield channel. In the **non-mycorrhizal** group, no β-glucuronidase activity nor arbuscles were observed, as expected. Whereas in the **mycorrhizal** group, arbuscles were observed in the three conditions, and β-glucuronidase activity was observed in the p240 and p700 groups, matching with arbuscle positions (see yellow and black arrows pointing arbuscle positions). This suggests that both the 240 bp region upstream of the ATG containing only the 4$^{th}$ CTTC motif and the 700 bp region containing the four CTTC motifs previously found in this work, are sufficient to drive *SlGRAS18* expression in arbuscule-containing cells.

In non-mycorrhizal composite tomato plants, no promoter activity was identified (Figure 9), except for the 700 bp fragment construct, for which eventually some blue staining was found primarily surrounding the central cylinder (see Figure S 4 in Annex 3). This result

is consistent with Ho-Plágaro et al. (2019), that described promoter activity of *SlGRAS18* restricted to cells surrounding the central cylinder and to the apical meristem in non-mycorrhizal composite plants for GUS reporter assay. Also on transgenic *A. thaliana* plants expressing the GUS gene under the control of the *AtSCL3* promoter in non-mycorrhizal conditions (since it is a non-host plant for AM symbiosis), Ito & Fukazawa (2021) showed that *AtSCL3* was expressed throughout the root system, with more density on root tips. As reported by Zhang et al. (2011), the AtSCL3 TF possesses a non-symbiotic role as a regulator of GA responses, which may explain the non-mycorrhizal-induced expression of *SlGRAS18*. This expression may require other regulatory elements found within the 700 bp fragment or even further upstream, which would explain why no non-AM-induced expression is observed in the 240 bp construct roots.

Likewise, no promoter activity was identified in mycorrhizal roots of the empty vector construct, as expected, since no regulatory region was fused. In addition, GUS-stained roots were counterstained with WGA-FITC to visualise fungal structures. Autofluorescence in the central cylinder, epidermal layer and root cell walls can be observed in every fluorescence image in Figure 9, as previously described by Ho-Plágaro et al. (2019). However, no fungal structures were found in non-mycorrhizal condition, showing that there was no cross-contamination.

Mycorrhizal roots of the 240 and 700 bp constructs showed GUS activity in the cortex zones affected by AM fungal root colonisation, mainly in arbuscule-containing cells, consistent with the results of Ho-Plágaro et al. (2019) and Avilés-Cárdenas et al. (2024). In Figure 9, the stronger blue stained dots of *GUS* expression are coincident with brightest zones of the fluorescent imaging, where arbuscules are found. This result confirms that colonisation by *R. irregularis* clearly activates *SlGRAS18* gene expression in arbusculated cells. This statement is also true in *M. truncatula*, where Mt*SCL3* expression is induced in arbuscule-containing cells during AM symbiosis (Seemann et al., 2022).

Blue staining and, therefore, GUS activity in both truncated promoters (240 bp and 700 bp) was mainly found in the cortex and central cylinder, even though it also seems to be extended to the epidermis in the 240 bp fragment construct. In the GUS reporter assay, the substrate X-Gluc is converted into a blue dye by the active β-glucuronidase, whereby the blue colour extends evenly over the entire root tissue. Thus, the staining of the epidermis layer may be due to a poor rinsing of the dye.

Only two vesicles were encountered in the whole analysis of mycorrhizal roots, meaning that arbuscles were not too old and degenerated. This matches with state of the arbuscules, being those highly branched and filling the entire plant cell.

This truncation analysis has revealed that both the 240 bp region upstream of the ATG containing only the 4$^{th}$ CTTC motif and the 700 bp region containing the four CTTC motifs previously found in this work, are sufficient to drive *SlGRAS18* expression in arbuscule-containing cells. This result suggests that the 4$^{th}$ CTTC motif, belonging to the 5'-UTR region of *SlGRAS18*, may play an important role in its regulation and expression under mycorrhizal conditions. In addition, the fact that no clear differences were observed between the 240 bp and the 700 bp fragments suggests that the 4$^{th}$ CTTC motif alone (without the other three CTTC motifs) is enough to trigger the AM-induced expression, whereas the additional motifs present in the 700 bp fragment may provide redundant or fine-tuning functions. Similar results were obtained by Heck et al. (2016) in a truncation analysis of a 230 bp region upstream of the ATG from the GRAS TF MIG1, in *M. truncatula*, obtaining a successful expression of MIG1 in mycorrhizal conditions. This 230 bp region also contained two CTTC motifs.

In a GUS reporter assay analysing the *LjPT4* promoter from *Lotus japonicus* with a mutation in the CTTC motif, Xue et al. (2018) obtained a significant reduction of *LjPT4* promoter activity, evidencing its requirement on the expression of this AM-induced phosphate transporter of the PAM. However, a residual *LjPT4* expression was detectable and confined to arbuscule-containing cells, suggesting the compensation of alternative redundant cis elements in transcriptional activation of *LjPT4* expression.

It should not be forgotten that these cis elements are regulatory precisely because TFs can bind to them and activate the transcription of the downstream gene. Recently, Paries et al. (2025) suggested that the differences in transactivation by different TFs that bind to cis elements are determined by the sequence context in which the cis elements reside, the distance among cis elements, and/or their distance to the transcriptional start site. They performed mutations in different CTTC motifs and AW-boxes (another cis-regulatory element) in the promoters of *PT4*, *RAM2* and *STR* AM-induced genes in *Nicotiana benthamiana* and observed activation by different TFs in each condition.

These findings underline the complexity of transcriptional regulation in AM-induced genes. Both the results of Xue et al. (2018) and Paries et al. (2025) suggest that the

compensation observed may not be only due to the presence of multiple CTTC motifs, but also to different TFs that can bind differentially depending on the position, distance, and sequence context of these motifs. This expands the line of investigation and suggests that future studies should focus not only on the regulatory sequences itself but also on the TFs that bind to them.

## 6. FUTURE PROSPECTS

To continue with the research focused on the AM-regulation of *SlGRAS18*, further experiments related with the 4$^{th}$ CTTC motif could provide valuable insights. For instance, performing an *A. rhizogenes*-mediated GUS reporter assay using both the 240 bp and 700 bp upstream fragments, but introducing specific mutations in the 4$^{th}$ CTTC motif, could help to further determine its role. In addition, it could be determined whether the other CTTC motifs take on the role or the 4$^{th}$ motif in its absence (due to the mutation). Similar analyses could be carried out for every CTTC motifs identified in this study, in order to observe whether they compensate for one another when one is disrupted. Additionally, it could be valuable to further research on the TFs that bind these regulatory motifs to gain a more holistic view of the regulation of *SlGRAS18*.

A point mutation in the CTTC motif, instead of a complete gene knock-out, would be preferred in these experiments, since *SlGRAS18* is also involved in non-mycorrhizal processes, such as GA signalling (Zhang et al., 2011). A knock-out would supress its basal expression, whereas a point mutation on this cis-regulatory motif would be expected to downregulate its AM-induced expression.

Genome-targeted editing of the CTTC motifs via CRISPR/Cas system would be required if mycorrhizal and physiological parameters need to be evaluated. Such a technique would allow the generation of plants with the same targeted mutation across all cells. Thus, it could be determined whether these mutations affect other parts of the plant.

Finally, this research could lead to a commercial crop with a downregulation on *SlGRAS18* AM-induced expression. Consequently, this plant, perhaps combined with a AMF-based biofertiliser, may develop a higher mycorrhization rate (Avilés-Cárdenas et al., 2024) and, therefore, be healthier, more vigorous and productive. The development of a genetically edited crop involves costs associated with research, validation and approval processes. Commercial viability would depend on market acceptance and

changes in legislation. In the European Union (EU), CRISPR-edited plants are currently regulated under the GMO (genetically modified organism) framework (Directive 2001/18/EC), meaning they require full approval and strict oversight. At the same time, the EU is negotiating a new legislation specifically for plants obtained by new genomic techniques, which could exempt CRISPR-edited plants from GMO legislation if they are comparable to conventionally bred varieties. The potential commercialization of such an edited cultivar would depend on whether and when these reforms are adopted.

## 7. CONCLUSIONS

The aim of the work was to further investigate the regulation of *SlGRAS18*, an AM-inducible GRAS TF in *S. lycopersicum* cv. Moneymaker. Thus, a truncation analysis using GUS reporter constructs fused to fragments upstream of the start codon from *SlGRAS18* of different lengths was conducted.

A manual analysis of the 2 kb upstream region of *SlGRAS18*, revealed the presence of four CTTC motifs, which are cis-regulatory elements associated with gene induction during AM colonisation. The 4$^{th}$ CTTC motif belongs to the 5'-UTR region of *SlGRAS18*, highlighting its potential regulatory relevance.

In transformed tomato roots, GUS activity was detected specifically in arbuscule-containing cortical cells in both constructs under mycorrhizal conditions, confirming that arbuscular mycorrhization activates *SlGRAS18* expression in arbusculated cells. The 240 bp fragment, containing only the 4th CTTC motif within the 5'-UTR, was sufficient to induce the expression of *SlGRAS18* in mycorrhizal conditions. Therefore, the 4$^{th}$ CTTC motif may play a central role in inducing *SlGRAS18* expression during AM symbiosis. Finally, the expression of β-glucuronidase or the mycorrhization did not notably impact shoot biomass under the tested conditions.

Overall, this study suggests that the 4$^{th}$ CTTC motif may play a crucial role in the regulation and expression of *SlGRAS18* under AM conditions. This contributes to a better understanding of the transcriptional regulation of *SlGRAS18*. In addition, since SlGRAS18 is known to be a negative regulator of AM symbiosis, it provides a potential tool for engineering plant gene expression under AM conditions in biotechnological applications, which could be able to enhance mycorrhization and, ultimately, lead to healthier and more productive crops. Nevertheless, more research needs to be done

focusing on the role of the 4th CTTC motif, as well as the other motifs found upstream of *SlGRAS18*.

## 8. BIBLIOGRAPHY

Ahmed, N., Li, J., Li, Y., Deng, L., Deng, L., Chachar, M., Chachar, Z., Chachar, S., Hayat, F., Raza, A., Umrani, J. H., Gong, L., & Tu, P. (2025). Symbiotic synergy: How Arbuscular Mycorrhizal Fungi enhance nutrient uptake, stress tolerance, and soil health through molecular mechanisms and hormonal regulation. *IMA Fungus*, *16*. https://doi.org/10.3897/imafungus.16.144989

Avilés-Cárdenas, J. D., Molinero-Rosales, N., Perez-Tienda, J., Rosas-Diaz, T., Castillo, A. G., & Garcia-Garrido, J. M. (2024). Enhancing arbuscular mycorrhiza symbiosis effectiveness through the involvement of the tomato GRAS transcription factor SCL3/SlGRAS18. *PLANT PHYSIOLOGY AND BIOCHEMISTRY*, *215*, 109019. https://doi.org/10.1016/j.plaphy.2024.109019

Bagal, D., Chowdhary, A. A., Mehrotra, S., Mishra, S., Rathore, S., & Srivastava, V. (2023). Metabolic engineering in hairy roots: An outlook on production of plant secondary metabolites. *Plant Physiology and Biochemistry*, *201*, 107847. https://doi.org/10.1016/j.plaphy.2023.107847

Barker, D. G., Chabaud, M., Russo, G., & Genre, A. (2017). Nuclear Ca2+ signalling in arbuscular mycorrhizal and actinorhizal endosymbioses: On the trail of novel underground signals. *New Phytologist*, *214*(2), 533–538. https://doi.org/10.1111/nph.14350

Bécard, G., & Fortin, J. A. (1988). Early events of vesicular–arbuscular mycorrhiza formation on Ri T-DNA transformed roots. *New Phytologist*, *108*(2), 211–218. https://doi.org/10.1111/j.1469-8137.1988.tb03698.x

Bennett, A. E., & Groten, K. (2022). The Costs and Benefits of Plant–Arbuscular Mycorrhizal Fungal Interactions. *Annual Review of Plant Biology*, *73*, 649–672. https://doi.org/10.1146/annurev-arplant-102820-124504

Brundrett, M. C., & Tedersoo, L. (2018). Evolutionary history of mycorrhizal symbioses and global host plant diversity. *New Phytologist*, *220*(4), 1108–1115. https://doi.org/10.1111/nph.14976

Cargill, R. I. M., Shimizu, T. S., Kiers, E. T., & Kokkoris, V. (2025). Cellular anatomy of arbuscular mycorrhizal fungi. *Current Biology*, *35*(11), R545–R562. https://doi.org/10.1016/j.cub.2025.03.053

Choi, J., Summers, W., & Paszkowski, U. (2018). Mechanisms Underlying Establishment of Arbuscular Mycorrhizal Symbioses. *Annual Review of Phytopathology*, *56*(1), 135–160. https://doi.org/10.1146/annurev-phyto-080516-035521

Custódio, V., Gonin, M., Stabl, G., Bakhoum, N., Oliveira, M. M., Gutjahr, C., & Castrillo, G. (2022). Sculpting the soil microbiota. *The Plant Journal*, *109*(3), 508–522. https://doi.org/10.1111/tpj.15568

Eurostat. (2024). *The fruit and vegetable sector in the EU - a statistical overview*. Retrieved August 12, 2025, from https://ec.europa.eu/eurostat/statistics-explained/index.php?title=The_fruit_and_vegetable_sector_in_the_EU_-_a_statistical_overview

Genre, A., Chabaud, M., Timmers, T., Bonfante, P., & Barker, D. G. (2005). Arbuscular Mycorrhizal Fungi Elicit a Novel Intracellular Apparatus in *Medicago truncatula* Root Epidermal Cells before Infection. *The Plant Cell*, *17*(12), 3489–3499. https://doi.org/10.1105/tpc.105.035410

Genre, A., Lanfranco, L., Perotto, S., & Bonfante, P. (2020). Unique and common traits in mycorrhizal symbioses. *Nature Reviews Microbiology*, *18*(11), 649–660. https://doi.org/10.1038/s41579-020-0402-3

Goralogia, G. S., Willig, C., & Strauss, S. H. (2025). Engineering *Agrobacterium* for improved plant transformation. *The Plant Journal*, *121*(5), e70015. https://doi.org/10.1111/tpj.70015

Heck, C., Kuhn, H., Heidt, S., Walter, S., Rieger, N., & Requena, N. (2016). Symbiotic Fungi Control Plant Root Cortex Development through the Novel GRAS Transcription Factor MIG1. *Current Biology*, *26*(20), 2770–2778. https://doi.org/10.1016/j.cub.2016.07.059

Ho-Plágaro, T., & García-Garrido, J. M. (2022a). Molecular Regulation of Arbuscular Mycorrhizal Symbiosis. *International Journal of Molecular Sciences*, *23*(11), 5960. https://doi.org/10.3390/ijms23115960

Ho-Plágaro, T., & García-Garrido, J. M. (2022b). Multifarious and Interactive Roles of GRAS Transcription Factors During Arbuscular Mycorrhiza Development. *Frontiers in Plant Science*, *13*, 836213. https://doi.org/10.3389/fpls.2022.836213

Ho-Plágaro, T., Huertas, R., Tamayo-Navarrete, M. I., Ocampo, J. A., & García-Garrido, J. M. (2018). An improved method for *Agrobacterium rhizogenes*-mediated transformation of tomato suitable for the study of arbuscular mycorrhizal symbiosis. *Plant Methods*, *14*(1). https://doi.org/10.1186/s13007-018-0304-9

Ho-Plágaro, T., Molinero-Rosales, N., Fariña Flores, D., Villena Díaz, M., & García-Garrido, J. M. (2019). Identification and Expression Analysis of GRAS Transcription Factor Genes Involved in the Control of Arbuscular Mycorrhizal Development in Tomato. *Frontiers in Plant Science*, *10*, 268. https://doi.org/10.3389/fpls.2019.00268

Ito, T., & Fukazawa, J. (2021). SCARECROW-LIKE3 regulates the transcription of gibberellin-related genes by acting as a transcriptional co-repressor of GAI-ASSOCIATED FACTOR1. *Plant Molecular Biology*, *105*(4), 463–482. https://doi.org/10.1007/s11103-020-01101-z

Jaiswal, V., Kakkar, M., Kumari, P., Zinta, G., Gahlaut, V., & Kumar, S. (2022). Multifaceted roles of GRAS transcription factors in growth and stress responses in plants. *iScience*, *25*(9). https://doi.org/10.1016/j.isci.2022.105026

Javot, H., Penmetsa, R. V., Breuillin, F., Bhattarai, K. K., Noar, R. D., Gomez, S. K., Zhang, Q., Cook, D. R., & Harrison, M. J. (2011). *Medicago truncatula mtpt4* mutants reveal a role for nitrogen in the regulation of arbuscule degeneration in arbuscular mycorrhizal symbiosis. *The Plant Journal*, *68*(6), 954–965. https://doi.org/10.1111/j.1365-313x.2011.04746.x

Jefferson, R. A., Kavanagh, T. A., & Bevan, M. W. (1987). GUS fusions: Beta-glucuronidase as a sensitive and versatile gene fusion marker in higher plants. *The EMBO Journal*, *6*(13), 3901–3907. https://doi.org/10.1002/j.1460-2075.1987.tb02730.x

Jote, C. (2023). The Impacts of Using Inorganic Chemical Fertilizers on the Environment and Human Health. *Organic and Medicinal Chemistry International Journal*, *13*, 008. https://doi.org/10.19080/OMCIJ.2023.13.555864

Kameoka, H., & Gutjahr, C. (2022). Functions of Lipids in Development and Reproduction of Arbuscular Mycorrhizal Fungi. *Plant and Cell Physiology*, *63*(10), 1356–1365. https://doi.org/10.1093/pcp/pcac113

Lynch, J. P., Strock, C. F., Schneider, H. M., Sidhu, J. S., Ajmera, I., Galindo-Castañeda, T., Klein, S. P., & Hanlon, M. T. (2021). Root anatomy and soil resource capture. *Plant and Soil*, *466*(1), 21–63. https://doi.org/10.1007/s11104-021-05010-y

Margulis, L. (1998). *Symbiotic Planet: A new look at evolution*. Basic Books.

Mauro, M. L., & Bettini, P. P. (2021). *Agrobacterium rhizogenes rolB* oncogene: An intriguing player for many roles. *Plant Physiology and Biochemistry*, *165*, 10–18. https://doi.org/10.1016/j.plaphy.2021.04.037

Murashige, T., & Skoog, F. (1962). A Revised Medium for Rapid Growth and Bio Assays with Tobacco Tissue Cultures. *Physiologia Plantarum*, *15*(3), 473–497. https://doi.org/10.1111/j.1399-3054.1962.tb08052.x

Neves, C., Ribeiro, B., Amaro, R., Expósito, J., Grimplet, J., & Fortes, A. M. (2023). Network of GRAS transcription factors in plant development, fruit ripening and stress responses. *Horticulture Research*, *10*(12), uhad220. https://doi.org/10.1093/hr/uhad220

Paniagua, R. (2011). *Citología e histología vegetal y animal.* (4th ed, Vol. 2). McGraw-Hill Interamericana.

Paries, M., Hobecker, K., Hernandez Luelmo, S., Binci, F., Guercio, A., Usländer, A., Cardoso, C., Si, Y., Wankner, L., Bashyal, S., Troycke, P., Brückner, F., Pimprikar, P., Shabek, N., & Gutjahr, C. (2025). The GRAS protein RAM1 interacts with WRI transcription factors to regulate plant genes required for arbuscule development and function. *Proceedings of the National Academy of Sciences*, *122*(21). https://doi.org/10.1073/pnas.2427021122

Pimprikar, P., & Gutjahr, C. (2018). Transcriptional Regulation of Arbuscular Mycorrhiza Development. *Plant and Cell Physiology*, *59*(4), 678–695. https://doi.org/10.1093/pcp/pcy024

Quandt, H.-J. (1993). Transgenic Root Nodules of *Vicia hirsuta:* A Fast and Efficient System for the Study of Gene Expression in Indeterminate-Type Nodules. *Molecular Plant-Microbe Interactions*, *6*(6), 699. https://doi.org/10.1094/mpmi-6-699

Rui, W., Mao, Z., & Li, Z. (2022). The Roles of Phosphorus and Nitrogen Nutrient Transporters in the Arbuscular Mycorrhizal Symbiosis. *International Journal of Molecular Sciences*, *23*(19), Article 19. https://doi.org/10.3390/ijms231911027

Salazar, Ó. (2023, January 30). *'From farm to table' | Healthier and more sustainable food system*. Euro-Funding. Retrieved July 23, 2025, from https://euro-funding.com/en/blog/from-farm-to-fork-healthy-and-sustainable-food-system/

Schenck, N., & Smith, G. (1982). Additional new and unreported species of mycorrhizal fungi (Endogonaceae) from Florida [*Glomus spp.*, *Gigaspora albida*]. *Mycologia*, *74*. https://agris.fao.org/search/en/providers/123819/records/64735f722c1d629bc97dcef5

Seemann, C., Heck, C., Voß, S., Schmoll, J., Enderle, E., Schwarz, D., & Requena, N. (2022). Root cortex development is fine-tuned by the interplay of MIGs, SCL3 and DELLAs during arbuscular mycorrhizal symbiosis. *New Phytologist*, *233*(2), 948–965. https://doi.org/10.1111/nph.17823

Shi, J., Wang, X., & Wang, E. (2023). Mycorrhizal Symbiosis in Plant Growth and Stress Adaptation: From Genes to Ecosystems. *Annual Review of Plant Biology*, *74*(1), 569–607. https://doi.org/10.1146/annurev-arplant-061722-090342

Shipunov, A. (2021). *Introduction to Botany*. Ori Books. https://herba.msu.ru/shipunov/school/biol_154/textbook/intro_botany.pdf

Smith, S. E., & Read, D. J. (2008). *Mycorrhizal symbiosis* (3rd ed). Academic Press.

St-Arnaud, M., Hamel, C., Vimard, B., Caron, M., & Fortin, J. A. (1996). Enhanced hyphal growth and spore production of the arbuscular mycorrhizal fungus *Glomus intraradices* in an *in vitro* system in the absence of host roots. *Mycological Research*, *100*(3), 328–332. https://doi.org/10.1016/S0953-7562(96)80164-X

Tharanath, A. C., Upendra, R. S., & Rajendra, K. (2024). Soil Symphony: A Comprehensive Overview of Plant–Microbe Interactions in Agricultural Systems. *Applied Microbiology*, *4*(4), Article 4. https://doi.org/10.3390/applmicrobiol4040106

Tóth, M., Tóth, Z. G., Fekete, S., Szabó, Z., & Tóth, Z. (2022). Improved and Highly Efficient Agrobacterium rhizogenes-Mediated Genetic Transformation Protocol: Efficient Tools for Functional Analysis of Root-Specific Resistance Genes for Solanum

lycopersicum cv. Micro-Tom. *Sustainability*, *14*(11), 6525. https://doi.org/10.3390/su14116525

Wang, X., Cheng, L., Xiong, C., Whalley, W. R., Miller, A. J., Rengel, Z., Zhang, F., & Shen, J. (2024). Understanding plant–soil interactions underpins enhanced sustainability of crop production. *Trends in Plant Science*, *29*(11), 1181–1190. https://doi.org/10.1016/j.tplants.2024.05.008

Xue, L., Klinnawee, L., Zhou, Y., Saridis, G., Vijayakumar, V., Brands, M., Dörmann, P., Gigolashvili, T., Turck, F., & Bucher, M. (2018). AP2 transcription factor CBX1 with a specific function in symbiotic exchange of nutrients in mycorrhizal *Lotus japonicus*. *Proceedings of the National Academy of Sciences of the United States of America*, *115*(39), E9239–E9246. https://doi.org/10.1073/pnas.1812275115

Young, J. M., Kuykendall, L. D., Martínez-Romero, E., Kerr, A., & Sawada, H. (2001). A revision of *Rhizobium* Frank 1889, with an emended description of the genus, and the inclusion of all species of *Agrobacterium* Conn 1942 and *Allorhizobium undicola* de Lajudie et al. 1998 as new combinations: *Rhizobium radiobacter, R. rhizogenes, R. rubi, R. undicola and R. vitis. International Journal of Systematic and Evolutionary Microbiology*, *51*(1), 89–103. https://doi.org/10.1099/00207713-51-1-89

Zhang, Z.-L., Ogawa, M., Fleet, C. M., Zentella, R., Hu, J., Heo, J.-O., Lim, J., Kamiya, Y., Yamaguchi, S., & Sun, T. (2011). Scarecrow-like 3 promotes gibberellin signaling by antagonizing master growth repressor DELLA in *Arabidopsis*. *Proceedings of the National Academy of Sciences of the United States of America*, *108*(5), 2160–2165. https://doi.org/10.1073/pnas.1012232108

## 9. SELF-ASSESSMENT

At the beginning of my internship, I found the topic quite complex. It took me some time to fully understand what I was working on. That is why I asked for scientific articles to read in order to gain a better understanding, even though they were not easy to comprehend at first. Luckily, during my first week, I had the opportunity to join a trial internship led by Diana, my supervisor, and directly related to my topic. It was a good start and introduction to the experimental techniques and concepts I was going to use. After many hours of reading and by asking Diana countless questions, I slowly started to

understand the topic better. Week after week, I became more confident, more engaged, and more comfortable with the work.

My stay was at a difficult time of year, as my supervisor went on holiday for a few days in August. Even so, this situation became an opportunity for me to develop more autonomously and gain confidence and trust my own judgement. It also made me realise that my supervisor had confidence in my work, even though she gave me guidance before she left and we worked out the next steps together. In addition, I could always count on trustworthy lab colleagues to turn to in case of doubts.

Another positive aspect was being able to carry out techniques that we had previously studied in class and that, when put into practice, made much more sense and I was able to understand them better and assimilate the reason for each step. Additionally, I could try other techniques than the ones used in this work, such as stable transformation, site-directed mutagenesis, and bacterial transformation using the heat shock method. These techniques were part of two other assays related to the topic that I performed in parallel to the experiment of this work, which I could not finish due to their long-term nature.

On a personal level, it was quite a challenge for me to live alone abroad. Even so, I consider it to have been a very enriching experience, both personally and professionally. Furthermore, it gave me the opportunity to practice my German with native people and learn more about their culture and traditions. I am very grateful to have been able to enjoy this opportunity and all that it has given me.

Finally, I am very excited about what I have learned during the course of this work. Fungi are a subject I am passionate about, and I find it fascinating to discover the mechanisms and regulation behind a “simple” symbiosis between two organisms. Furthermore, I am impressed to see how these often invisible underground microorganisms can play a key role in making agriculture more sustainable. All this knowledge gained, both from experimental work and from reading and studying articles, is and will be very valuable to me. In fact, I will already start to apply it in my immediate future, since I have had the opportunity to start working in a company dedicated to biofertilisers based on microorganisms, a field in which I want to continue to deepen.

# ANNEX 1

Unlike AM symbioses, the hyphae of ECM fungi do not penetrate root cells but develop between the epidermal cells. This intercellular hyphal network is known as the Hartig net (Figure S 1) and is where nutrient exchange takes place. In addition, ECM fungi form a mantle, a fungal sheath that envelops the root. This type of mycorrhiza is found on about 2% of terrestrial plant species, almost exclusively on woody shrubs and trees. Many ECM fungi are partly saprophytic, being able to decompose organic matter and contribute to nutrient cycling (Genre et al., 2020; Shi et al., 2023).

Ericoid mycorrhizal (ERM) symbiosis relationships are the least diverse in terms of plant and fungal species. They are limited to plants in the family Ericaceae and Diapensiaceae represented approximately 1.4% of terrestrial plant species. Ericoid mycorrhizal fungi colonise individual epidermal cells from the root surface, forming densely intracellular coils (Figure S 1) where nutrient exchange takes place. These fungi include diverse lineages of Ascomycota (e.g. Helotiales, Chaetothyriales) as well as some Basidiomycota (Brundrett & Tedersoo, 2018; Genre et al., 2020; Shi et al., 2023).

Orchid mycorrhizas (ORM) are restricted to the plant family Orchidaceae and account for about 10% of terrestrial plant species. Similar to ericoid mycorrhizas, ORM are even more committed to assisting the host plant through their carbon nutrition. Since orchid seeds are tiny and have limited nutrition stores, the seedling stage is typically obligately mycorrhizal. Fungi producing ORM symbiosis belong to the genus *Rhizoctonia*, in the phylum Basidiomycota. These fungi form highly coiled hyphal structures in the root cortex cells known as pelotons (Figure S 1). Once mature, these pelotons are digested by the host plant (Brundrett & Tedersoo, 2018; Genre et al., 2020; Shi et al., 2023).

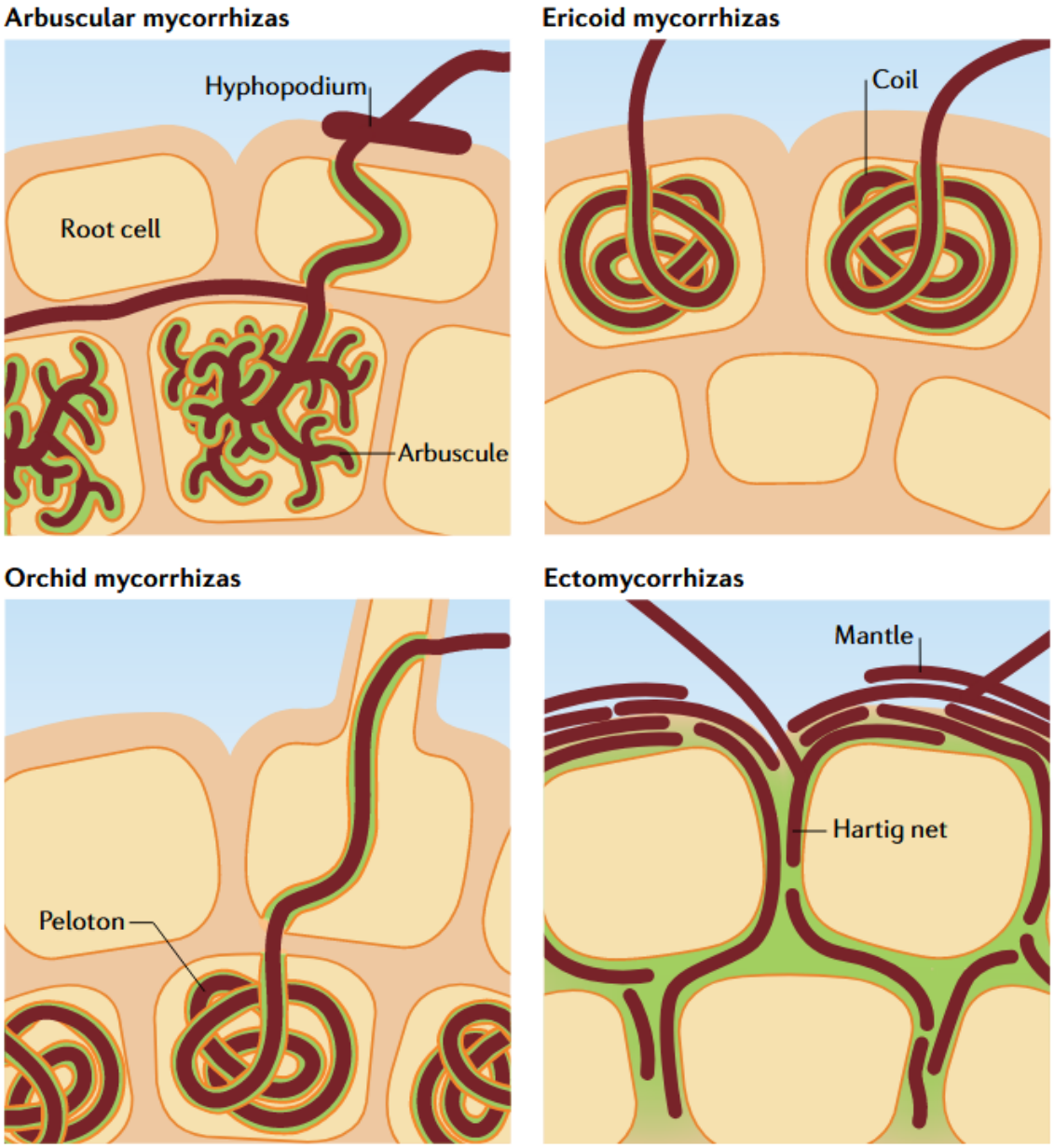


**Figure S 1.** The four main types of mycorrhizas: arbuscular mycorrhizas (AM), ericoid mycorrhizas (ERM), orchid mycorrhizas (ORM), and ectomycorrhizas (ECM). In AM, hyphae originating from soil-germinating spores contact the epidermal cells of host lateral roots through a specialised lobed structure called the hyphopodium. Then, hyphae cross the epidermal layer and reach the inner cortical cells, where highly branched tree-like hyphal structures, known as arbuscules, are formed. In ERM, hyphae penetrate the thick epidermal cell walls of Ericaceae roots and dense hyphal coils are then produced inside each epidermal cell. In the case of ORM, hyphae penetrate epidermal cells and reach the cortical parenchyma, where they form large hyphal coils, called pelotons. In ECM, symbiotic fungi form a mantle, a fungal sheath that envelops the whole root tip. The mantle's inner hyphae further develop between epidermal cells, reaching different depths into the cortical tissue (depending on the host plant). Such intraradical hyphae never penetrate the cell lumen and conform the so-called Hartig net. From Genre et al. (2020).

# ANNEX 2

## Media and solutions compositions

### MS medium (Murashige & Skoog, 1962)

The components of MS medium listed in Table S 1 were dissolved in $dH_2O$, the pH was adjusted to 5.7, the appropriate amount of agar was added, and the solution was autoclaved.

**Table S 1.** Composition of MS medium.

| Component | Final concentration | Component | Final concentration |
|---|---|---|---|
| **Macronutrients** | | **Micronutrients** | |
| $CaCl_2 \cdot 2\ H_2O$ | 0.45 g/L | $CoCl_2 \cdot 6\ H_2O$ | 0.03 mg/L |
| $KH_2PO_4$ | 0.17 g/L | $CuSO_4 \cdot 5\ H_2O$ | 0.03 mg/L |
| $KNO_3$ | 1.90 g/L | $H_3BO_3$ | 6.20 mg/L |
| $MgSO_4 \cdot 7\ H_2O$ | 0.37 g/L | KI | 0.83 mg/L |
| $NH_4NO_3$ | 1.65 g/L | $MnSO_4 \cdot H_2O$ | 16.90 mg/L |
| **Vitamins** | | $Na_2MoO_4 \cdot 2\ H_2O$ | 0.25 mg/L |
| myo-Inositol | 100 mg/L | $ZnSO_4 \cdot 7\ H_2O$ | 8.60 mg/L |
| Nicotinic acid | 1 mg/L | **Na-FeEDTA** | 36 mg/L |
| Pyridoxine · HCl | 1 mg/L | **Sucrose** | 30 g/L |
| Thiamine · HCl | 10 mg/L | | |

The table shows the final concentrations of macro- and micronutrients, vitamins, and other components in the MS medium used in this experiment, which has been slightly modified from the original MS medium (Murashige & Skoog, 1962). All concentrations are expressed per litter of medium. NaFe-EDTA is listed separately due to its chelated nature and independent stock preparation, although iron is considered a micronutrient. This formulation was used as a base medium without sugar, or sugar and vitamins, in *A. rhizogenes*-mediated transformation (see chapter 4.3).

### 0.5x Hoagland solution (Javot et al., 2011)

All the components of 0.5x Hoagland solution listed in Table S 2 were dissolved in dH2O and the pH was adjusted to 6.1. The Hoagland nutrient solution in 0.5x concentration contains 15 mM of nitrogen and 50 µM of inorganic phosphate. The composition is based on supplementary table 2 of Javot et al. (2011).

**Table S 2.** Composition of 0.5x Hoagland solution.

| Component | Final concentration (0.5x) | Component | Final concentration (0.5x) |
|---|---|---|---|
| **Macronutrients** | | **Micronutrients** | |
| $Ca(NO_3)_2 \cdot 2\ H_2O$ | 0.82 g/L | $CoCl_2 \cdot 6\ H_2O$ | 0.048 mg/L |
| $KH_2PO_4$ | 6.81 mg/L | $CuSO_4 \cdot 5\ H_2O$ | 0.124 mg/L |
| $KNO_3$ | 0.51 g/L | $H_3BO_3$ | 0.618 mg/L |
| $MgSO_4 \cdot 7\ H_2O$ | 0.25 g/L | $MnCl_2 \cdot 4\ H_2O$ | 0.396 mg/L |
| **HCl** | 0.91 mg/L | $Na_2MoO_4 \cdot 2\ H_2O$ | 0.048 mg/L |
| **MES buffer** | 97.60 mg/L | $ZnSO_4 \cdot 7\ H_2O$ | 0.288 mg/L |
| **NaFe-EDTA** | 18.35 mg/L | | |

The table shows the final concentrations of macro- and micronutrients, and other components in Hoagland fertiliser solution (Javot et al., 2011). All concentrations are expressed per litter of medium. NaFe-EDTA is listed separately due to its chelated nature and independent stock preparation, although iron is considered a micronutrient. This solution was used to fertilize mycorrhizal and non-mycorrhizal potted plants (see chapter 4.4).

**Minimal (M) medium** (Bécard & Fortin, 1988)

The components of M medium listed in Table S 3, except for Phytagel®, were dissolved in $dH_2O$, the pH was adjusted to 5.5, Phytagel® was added, and the solution was autoclaved.

**Table S 3.** Composition of Minimal (M) medium.

| Component | Final concentration | Component | Final concentration |
|---|---|---|---|
| **Macronutrients** | | **Vitamins** | |
| $Ca(NO_3)_2 \cdot 2\ H_2O$ | 288 mg/L | Glycine | 3 mg/L |
| KCl | 65 mg/L | myo-Inositol | 50 mg/L |
| $KH_2PO_4$ | 4.80 mg/L | Nicotinic acid | 0.5 mg/L |
| $KNO_3$ | 80 mg/L | Pyridoxine · HCl | 0.1 mg/L |
| $MgSO_4 \cdot 7\ H_2O$ | 731 mg/L | Thiamine · HCI | 0.1 mg/L |
| **Micronutrients** | | **NaFe-EDTA** | 8 mg/L |
| $CuSO_4 \cdot 5\ H_2O$ | 0.13 mg/L | **Phytagel®[1] 0.3%** | 3 g/L |
| $H_3BO_3$ | 1.50 mg/L | **Sucrose** | 10 g/L |
| $MnCl_2 \cdot 4\ H_2O$ | 6 mg/L | | |
| $Na_2MoO_4 \cdot 2\ H_2O$ | 2.40 µg/L | | |
| $ZnSO_4 \cdot 7\ H_2O$ | 2.65 mg/L | | |

The table shows the final concentrations of macro- and micronutrients, vitamins, and other components in the M medium (Bécard & Fortin, 1988). All concentrations are expressed per litter of medium. NaFe-EDTA is listed separately due to its chelated nature and independent stock preparation, although iron is considered a micronutrient. Although glycine is not a vitamin itself, it is commonly included under the vitamin mix of plant tissue culture media due to its grow-promoting effects. The M medium was used for *in vitro* cultivation of Ri-transformed *Daucus carota* roots mycorrhizal with the AMF *Rhizophagus irregularis* (see chapter 4.5). [1] Phytagel® (Sigma-Aldrich, St. Louis, MO, USA).

# ANNEX 3

## Supplementary figures

**Figure S 2.** Harvested composite tomato plants after rinsing the roots with distilled water.

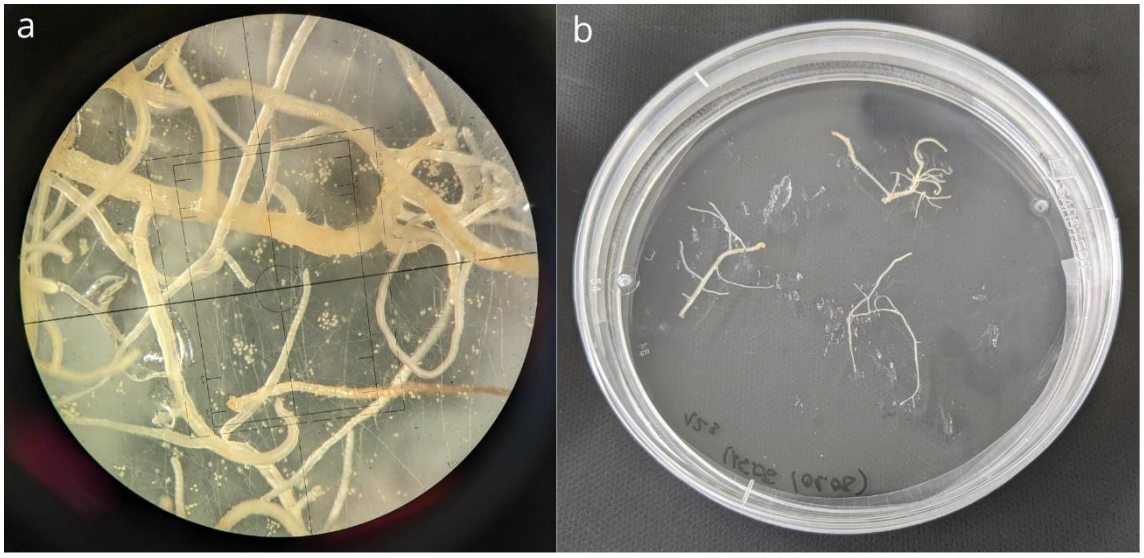


**Figure S 3.** Propagation of AMF *R. irregularis* through Ri-transformed Daucus carota roots. (a) Old mycorrhizal carrot roots observed under bright-field microscopy. Mycelium as well as spore clusters can be observed. (b) Freshly transferred carrot root segments on new M medium Petri dishes.

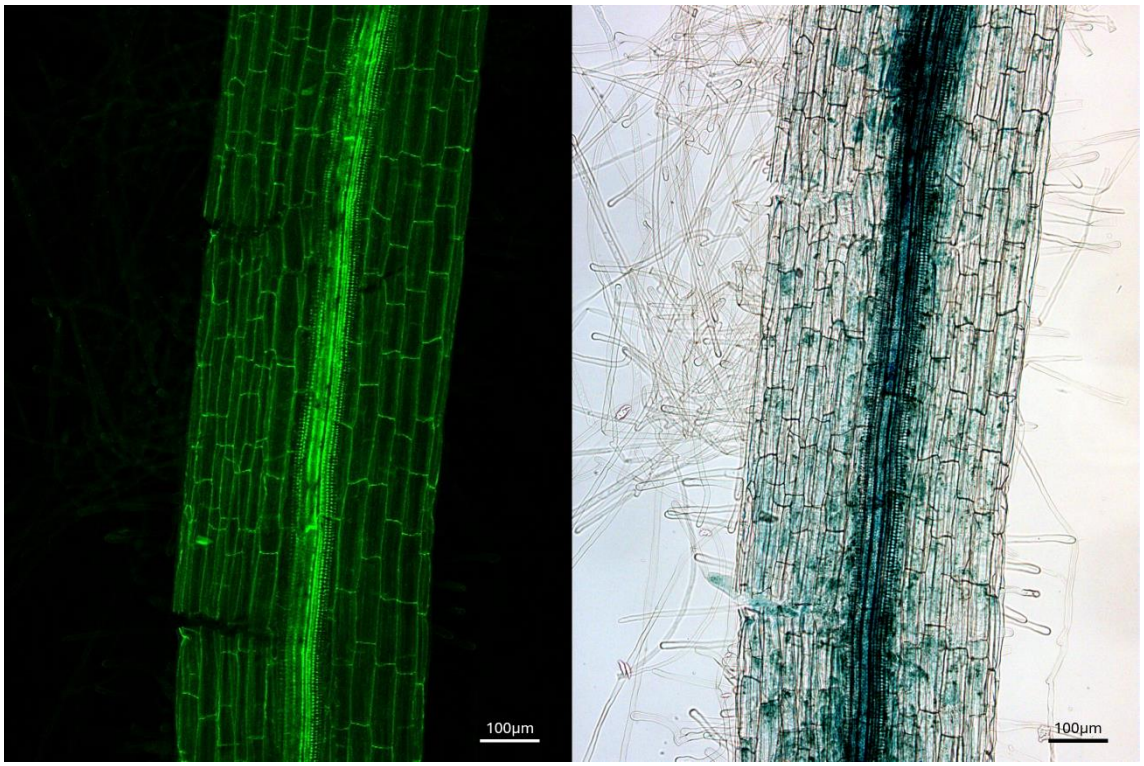


**Figure S 4.** Truncation analysis of the *SlGRAS18* promoter activity in *A. rhizogenes*-transformed *S. lycopersicum* roots after GUS staining and WGA-FITC counterstaining. GUS activity in transformed roots expressing pGFPGUS-RedRoot fused to a 700 bp fragment upstream of ATG start codon from *SlGRAS18* was assessed after 5 weeks of inoculation with *R. irregularis*. The left image shows the FITC channel in order to visualise WGA-FITC counterstaining of fungus structures, and the right image shows the brightfield channel for visualising GUS staining and, therefore, promoter activity. No fungal structures are observed in the FITC channel, whereas blue staining is observed in the central cylinder, indicating a possible non-AM induced expression of the β-glucuronidase.

# ANNEX 4

## Statistical data

**Table S 4.** Shapiro–Wilk test of normality for shoot fresh weight data across all samples and within experimental subgroups: mycorrhizal (M), non-mycorrhizal (NM), empty vector (pEV), 240 bp fragment upstream of the start codon from *SlGRAS18* (p240), 700 bp fragment upstream of the start codon from *SlGRAS18* (p700). Since for all the subgroups p>0.05, the distribution is not significantly different from a normal distribution and is therefore considered that all experimental subgroups possess a normal distribution.

| Group | W statistic | df | p-value |
|---|---|---|---|
| **Weight** | 0.96 | 30 | 0.29 |
| **M** | 0.94 | 17 | 0.35 |
| **NM** | 0.95 | 13 | 0.65 |
| **pEV** | 0.88 | 9 | 0.14 |
| **p240** | 0.92 | 12 | 0.31 |
| **p700** | 0.96 | 9 | 0.78 |

**Table S 5.** Levene's test for equality of variances in shoot fresh weight. This table shows the F statistic (Levene's statistic), degrees of freedom (df1, df2), and p-values from Levene's test, used to evaluate whether the variance in shoot fresh weight is homogeneous across the experimental groups. The assumption of homogeneity of variances is met (p>0.05), therefore, the variances are homogeneous.

| Levene's test | F | df1 | df2 | p-value |
|---|---|---|---|---|
| **Weight** | 0.13 | 1 | 28 | 0.718 |

**Table S 6.** Two-way ANOVA for shoot fresh weight data. This table summarizes the results of a two-way ANOVA testing the effects of construct type, mycorrhiza treatment, and their interaction on shoot fresh weight. It shows the sum of squares (SS), degrees of freedom (df), mean square (MS), F statistic, and p-value. Since p>0.05 in all sources of variation, no significant differences in shoot fresh weight were observed between constructs or mycorrhizal conditions, nor was there a significant interaction between these two factors.

| Source | SS | df | MS | F | p-value |
|---|---|---|---|---|---|
| **Mycorrhiza** | 530.10 | 1 | 530.10 | 0.01 | 0.925 |
| **Construct** | 15798.52 | 2 | 7899.26 | 0.13 | 0.875 |
| **Interaction** | 6413.84 | 2 | 3206.92 | 0.05 | 0.947 |
| **Error** | 1412363 | 24 | 58848.45 | | |

**Table S 7.** One-way ANOVA for shoot fresh weight across six experimental groups. This table shows the results of a one-way ANOVA comparing shoot fresh weight among the six experimental combinations of construct and mycorrhiza treatments. It shows the sum of squares (SS), degrees of freedom (df), mean square (MS), F statistic, and p-value. Since p>0.05 variation, there are no significant differences in shoot fresh weight between the six experimental groups

| Source | SS | df | MS | F | p-value |
|---|---|---|---|---|---|
| **Between groups** | 23197.12 | 5 | 4639.42 | 0.08 | 0.995 |
| **Within groups** | 1412363 | 24 | 58848.45 | | |
| **Total** | 1435560 | 29 | | | |

**Table S 8.** Fisher's Least Significant Difference (LSD) post-hoc test for shoot fresh weight. This table lists all pairwise comparisons between experimental groups from the one-way ANOVA, showing mean differences (Group 1 – Group 2), standard error of the difference and p-values. The abbreviations stand for mycorrhizal (M), non-mycorrhizal (NM), empty vector (EV), 240 bp fragment upstream of the start codon from *SlGRAS18* (240), 700 bp fragment upstream of the start codon from *SlGRAS18* (700). None of the comparisons reached statistical significance at $p < 0.05$, meaning that there is no significant difference between any of the groups.

| Group 1 | Group 2 | Mean difference | Standard error | p-value |
|---|---|---|---|---|
| **M EV** | **M 240** | -52.34 | 142.04 | 0.716 |
| **M EV** | **M 700** | -6.62 | 153.43 | 0.966 |
| **M EV** | **NM EV** | 32.77 | 162.73 | 0.842 |
| **M EV** | **NM 240** | -25.02 | 153.43 | 0.872 |
| **M EV** | **NM 700** | -41.05 | 162.73 | 0.803 |
| **M 240** | **M 700** | 54.72 | 142.04 | 0.750 |
| **M 240** | **NM EV** | 85.12 | 152.05 | 0.581 |
| **M 240** | **NM 240** | 27.32 | 142.04 | 0.849 |
| **M 240** | **NM 700** | 11.29 | 152.05 | 0.941 |
| **M 700** | **NM EV** | 39.39 | 162.73 | 0.811 |
| **M 700** | **NM 240** | -18.40 | 153.43 | 0.906 |
| **M 700** | **NM 700** | -34.43 | 162.73 | 0.834 |
| **NM EV** | **NM 240** | -57.79 | 162.73 | 0.726 |
| **NM EV** | **NM 700** | -73.82 | 171.53 | 0.671 |
| **NM 240** | **NM 700** | -16.03 | 162.73 | 0.922 |

**Table S 9.** Raw shoot fresh weight data for all experimental plants. This table presents the original shoot fresh weight measurements (in mg) for each plant, organized by construct and mycorrhiza treatment.

| Plant ID | Construct | Mycorrhiza | Weight (mg) |
|---|---|---|---|
| **1** | Mycorrhizal | Empty vector | 1022 |
| **2** | Mycorrhizal | Empty vector | 310 |
| **3** | Mycorrhizal | Empty vector | 954 |
| **4** | Mycorrhizal | Empty vector | 776.3 |
| **5** | Mycorrhizal | Empty vector | 319.2 |
| **6** | Mycorrhizal | 240 bp promoter fragment | 682.1 |
| **7** | Mycorrhizal | 240 bp promoter fragment | 956.9 |
| **8** | Mycorrhizal | 240 bp promoter fragment | 984.8 |
| **9** | Mycorrhizal | 240 bp promoter fragment | 713.6 |
| **10** | Mycorrhizal | 240 bp promoter fragment | 593.1 |
| **11** | Mycorrhizal | 240 bp promoter fragment | 651.1 |
| **12** | Mycorrhizal | 240 bp promoter fragment | 518.9 |
| **13** | Mycorrhizal | 700 bp promoter fragment | 610.1 |
| **14** | Mycorrhizal | 700 bp promoter fragment | 619.5 |
| **15** | Mycorrhizal | 700 bp promoter fragment | 431.9 |
| **16** | Mycorrhizal | 700 bp promoter fragment | 814.5 |
| **17** | Mycorrhizal | 700 bp promoter fragment | 938.6 |
| **18** | Non-mycorrhizal | Empty vector | 964.2 |
| **19** | Non-mycorrhizal | Empty vector | 166.6 |
| **20** | Non-mycorrhizal | Empty vector | 550.2 |
| **21** | Non-mycorrhizal | Empty vector | 893.1 |
| **22** | Non-mycorrhizal | 240 bp promoter fragment | 616.7 |
| **23** | Non-mycorrhizal | 240 bp promoter fragment | 433.4 |
| **24** | Non-mycorrhizal | 240 bp promoter fragment | 714.1 |
| **25** | Non-mycorrhizal | 240 bp promoter fragment | 1009.2 |
| **26** | Non-mycorrhizal | 240 bp promoter fragment | 733.2 |
| **27** | Non-mycorrhizal | 700 bp promoter fragment | 609.2 |
| **28** | Non-mycorrhizal | 700 bp promoter fragment | 677.2 |
| **29** | Non-mycorrhizal | 700 bp promoter fragment | 787.7 |
| **30** | Non-mycorrhizal | 700 bp promoter fragment | 795.3 |